3.1.7. – stateczność
2.2.1. – mechanika punktu i układu nieodkształcalnych

K. Janicki, W. Szemplińska-Stupnicka

STABILITY OF SUBHARMONICS AND ESCAPE PHENOMENA IN THE TWIN-WELL POTENTIAL DUFFING SYSTEM

6/1993

WARSZAWA 1993

ISSN 0208-5658

Praca wpłynęła do Redakcji dnia 27 stycznia 1993 r.

Na prawach rękopisu

Instytut Podstawowych Problemów Techniki PAN
Nakład 100 egz. Ark.wyd. 3,50 Ark.druk.4,25
Oddano do drukarni w lutym 1993 r.

Wydawnictwo Spółdzielcze sp. z o.o.
Warszawa, ul.Jasna 1

Krzysztof Janicki
Wanda Szemplińska-Stupnicka
Samodzielna Pracownia Dynamiki Stosowanej

STABILITY OF SUBHARMONICS AND ESCAPE PHENOMENA IN THE TWIN-WELL POTENTIAL DUFFING SYSTEM

ABSTRACT

Low order subharmonic resonances in the twin-well potential Duffing system are studied: 1:1, 1:2, 1:3 of one-well motion and 1:1, 1:3 of cross-well motion. Solutions for the resonances are found using a modification of the near-linear perturbation method. Then Hill's variational equation allows us to examine stability of the solutions. Due to the above methods major bifurcations of subharmonics can be located approximately in the parameter space: folds, period-doublings and symmetry-breakings.

Results of numerical experiment are included for comparison. They show that the analysis of the local bifurcations can estimate phenomena of escape from potential well. Two types of chaotic attractor catastrophes are also found in the system: one is invertible with respect to parameter changes, the other is not and involves hysteresis. The former type seems to be related to the local bifurcations of regular orbits, the latter corresponds to the boundary crisis.

1. Introduction

The Duffing equation with negative stiffness:

$$\ddot{x} + h\dot{x} - \alpha x + \beta x^3 = F\cos\nu t \ , \qquad (1)$$

$$h,\alpha,\beta > 0 \ , \qquad T \equiv \frac{2\pi}{\nu}$$

has been an object of detailed studies in nonlinear dynamics during last years. Initially it was investigated as a simplified

mathematical description of buckled beam vibrations (Holmes [1], Holmes, Moon [2], Tang, Dowell [3], Moon and Holmes [4]) or plasma oscillations (Mahaffey [5]). Its most intuitive mechanical model is, however, the device depicted in Fig 1: a particle moving alongside walls of a twin-well potential, with the base driven sinusoidally. Let the particle move initially in one of the wells. Certain changes of parameters of (1) (ie a smooth increase of the excitation amplitude F) may result in a sudden transition from one-well to cross-well motion (regular or chaotic). This phenomenon is referred to as escape. Throughout this paper all one-well motions are called Small Orbit motions and cross-well motions Large Orbit motions.

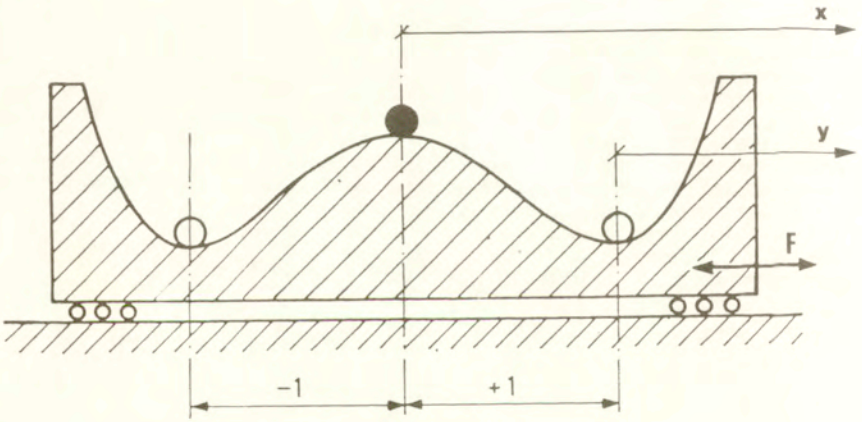

Fig. 1. A mechanical model of the twin-well Duffing system

The meaning of (1) goes far beyond its physical applications. Nowadays it becomes an archetypal model for studying universal features of nonlinear systems, concerning highly regular, periodic solutions, as well as complicated chaotic motions (Guckenheimer, Holmes [6], Wiggins [7]). Below we provide a short review of basic methods and results concerning (1).

Many theoretical results are obtained in terms of dissipative perturbation of a nonlinear, integrable Hamiltonian system and studied further using the technique of Poincare maps. (Greenspan, Holmes [8], also [1], [6], [7]). The existence of a saddle homoclinic point in the phase space is relevant to this approach. The Melnikov theory provides us ia with the general picture of the phase space of (1) under increasing perturbation and predicts the appearance of subharmonics and the homoclinic bifurcation (tangling) of invariant manifolds of the saddle point. The latter implies that for large enough perturbations an extremely complicated structure arises in the phase space, containing orbits of all periods and nonperiodic dense orbits. This result is obtained by associating a two dimensional diffeomorphism of the Smale horseshoe type with the flow.

The behavior of invariant manifolds under perturbation is also essential to the chaotic transport theory (Wiggins [9]) and probability phenomena (Neihstadt [10]) in the phase space.

The complicated nonperiodic orbits, which arise in the homoclinic bifurcations may be attracting or not. If they are, they can be observed in numerical experiment and numerical integration allows us to estimate Hausdorff-like metrical dimensions, Lyapunov exponents, Fourier spectra or other characteristics of the chaotic attractors (Ueda [11], Moon, Li [12], Arecchi,Lisi [13], Gafka,Tani [14]). If they are not attracting, they can not be observed directly in numerical simulations but they still influence the dynamics of (1), being responsible for complicated transient motions (so called transient chaos). The homoclinic bifurcations are also connected with bifurcations of basins of attraction of periodic and chaotic motions and their fractal properties. Such study is usually accompanied by detailed numerical research (Moon, Li [15], Ueda et al [16], Pezeshki and Dowell [17]).

This paper follows the line of yet another approach, involving classical approximate methods like harmonic balance or near-linear perturbation techniques. These methods are used to find regular solutions. Then certain conditions are imposed on

the solutions referred to as "escape criteria" - approximate criteria for the transition from one-well motions to other types of motions. Validity of such criteria is then justified using numerical experiment. We find relationships between the escape phenomena and some instabilities of periodic solutions (Szemplińska-Stupnicka [18], Szemplińska-Stupnicka and Rudowski [19,20]). Similar ideas, although based on near-Hamiltonian, not near-linear approach, are discussed in McRobie and Thompson [21].

In this paper we investigate the subharmonic region of frequencies of (1). Despite intensive studies of the Duffing system this parameter region has not been yet examined numerically except partial studies of basin bifurcations in (F,h) parameter plane for constant forcing frequency and for large disturbances [16]. We fill the gap, providing also numerical verification for the results of Melnikov theory. In order to clarify some phenomena not understood in Melnikov approach we develop the near-linear perturbation method.

We study subharmonic resonances of:

- Large Orbit (cross-well motion - we write shortly LO) of order 1:1, 1:3 (ie motions of period T and 3T, where T is the period of external forcing)
- Small Orbit (one-well motion - we write SO) of order 1:1, 1:2, 1:3 (ie orbits of period T, 2T, 3T respectively).

Our parameter space is the plane (ν,F). We keep constant coefficients $\alpha=0.5$, $\beta=0.5$ (this is the normalized form, considered eg in [12], [15], [17], [18-20]) and damping $h=0.1$. Our aim is to give an overall picture of bifurcations in this region. Phenomena close to the tangling corresponding to Melnikov homoclinic function, which includes creation and further bifurcations of higher order subharmonics, are not the subject of this study, because they appear in very narrow parameter regions.

In theoretical analysis we use KBM (Krylov - Bogoliubov - Mitropolsky) perturbation method. The method provides us with periodic solutions and allows us to examine their stability. We

follow the approach presented earlier in [18-20], although in this paper we modify the classic perturbation technique in order to investigate subharmonic Large Orbit vibrations.

The stability analysis associated with the perturbation method allows us to find the instabilities which consist in the build-up of the same harmonics in disturbance as the Fourier components of the solution itself (see sec 2.1). The experiment shows, however, also other type instabilities, which consist in the build-up of new harmonic components. By means of variational Hill's equation the class of instabilities can be examined. We focus on:

- period doubling instability
- symmetry breaking instability.

The above methods allow us to predict major bifurcations observed in the subharmonic region of frequencies: folds, period doublings and symmetry-breakings. We want to underline at this point that only fold bifurcations of subharmonic solutions of (1) have been found so far using Melnikov approach (see [6-8]). We refer to this problem further in section 4.

Theoretical results are compared with numerical experiment. In numerical analysis we use the "brute force" approach - simple Runge-Kutta integration of the system (1), meaning that only stable solutions can be found in computer simulations and compared with the theory. Thus in both theoretical and experimental investigations we confine ourselves only to bifurcations of stable solutions.

Numerical simulations indicate, that every escape corresponds to a certain type instability of a Small Orbit motion. Indeed, if for a given point in (ν,F) parameter plane all possible SO motions are unstable we can have only Large Orbit motions stable in this point. Thus the points where the last SO has lost stability correspond to escape phenomena in the parameter space.

The idea lying behind our work is that in the region of parameters considered we can confine ourselves only to examining stability of a few low-order subharmonics. Assuming this we can state that stability analysis of approximate solutions can

locate escape phenomena in the parameter space.

As another result of experimental investigations we discuss sudden destructions of the chaotic attractor. The phenomena are referred to as blue-sky catastrophes (Abraham, Stewart [22]) and their studies are usually based on the concept of crisis - the collision between the chaotic attractor and an unstable orbit on its basin boundary. This collision is in fact the homoclinic bifurcation of stable and unstable manifolds of the unstable orbit (Grebogi, Ott, Yorke [23,24]). The crisis-type bifurcations are observed in our experiments. In addition, another type of the blue-sky catastrophe has been found - it involves stable periodic orbits appearing suddenly within the basin of the chaotic attractor and replacing the attractor. The scenario is rather of subduction, than crisis type (cf [23]). Due to local bifurcations involved the latter phenomenon can be located approximately in the parameter space using perturbation theory.

2. Approximate solutions

2.1 The perturbation method

Perturbation methods for nonlinear oscillators can often be classified as either near-Hamiltonian or near-linear. The former use integrable Hamiltonian system as a zeroth approximation, the latter start with linear systems. We will use a near-linear method starting with harmonic oscillator in the zeroth approximation. Thus we consider equations of the form:

$$\ddot{x} + \Omega^2 x + \mu f(x,\dot{x},\nu t) = 0 \quad , \tag{2.a}$$

or

$$\ddot{x} + \Omega^2 x + \mu f(x,\dot{x},\nu t) + \mu^2 g(x,\dot{x},\nu t) = 0 \quad , \tag{2.b}$$

with Ω^2 not depending on x, $\dot{x}$, t and f, g - 2π periodic in νt.

We will choose the form (2.a) for Large Orbit and (2.b) for Small Orbit case - see sec. 2.2, 2.3.

We use the perturbation method in the resonant version (Szemplińska-Stupnicka [25]) ie we first transform (2.a), (2.b) to the form:

$$\ddot{x} + \omega^2 x + \mu(f+\sigma x) = 0 \qquad (3.a)$$

or

$$\ddot{x} + \omega^2 x + \mu f + \mu^2(g+\sigma x) = 0 \ , \qquad (3.b)$$

where: $\omega = n\nu/m$ with n, m integers relatively prime.

Here an important assumption have been made, that:

$$\Omega^2 - \omega^2 = \mu\sigma \qquad \text{for (3.a)} \qquad (4.a)$$

or

$$\Omega^2 - \omega^2 = \mu^2\sigma \qquad \text{for (3.b)} \ , \qquad (4.b)$$

with $\sigma = O(1)$ - detuning parameter. Note that eqs (4) confine the region of frequencies ν considered to these which are close to $m\Omega/n$.

Now we seek solutions of eqs (3) in the form

$$x(t) = a\cos\upsilon + \mu x_1(a,\varphi,t) + \mu^2 x_2(a,\varphi,t) + \ldots \ , \qquad (5)$$

where $\upsilon = \omega t + \varphi$,
with "slowly varying" amplitude and phase:

$$\dot{a} = \mu M_1(a,\varphi) + \mu^2 M_2(a,\varphi) + \ldots \ , \qquad (6.a)$$

$$\dot{\varphi} = \mu N_1(a,\varphi) + \mu^2 N_2(a,\varphi) + \ldots \ , \qquad (6.b)$$

with M_i, N_i $(i=1,2\ldots)$ 2π periodic in φ - unknown coefficients to be determined.

Following classical terminology of the perturbation literature we will use the term resonance referring to the relations (4) ie depending on the parameters region under investigation. The n:m resonance means here that we are in the region of driving frequencies ν close to $m\Omega/n$ and expect almost

sinusoidal response (5) with dominating frequency $\omega=n\nu/m$. This does not imply always that the period of the periodic orbit appearing in n:m resonance is defined by the frequency ω. For example the 2:1 resonance means here that the response has the dominating frequency 2ν, but the component with frequency 1ν also appears in the solution (see [19]) causing the orbit to be 1T periodic, not T/2 periodic (T is the period of external force). In near-Hamiltonian approach resonances are understood in slightly different sense: in n:m resonance mT/n periodic orbits of the unperturbed Hamiltonian system are considered and their behavior under perturbation is studied. The orbits which are preserved in the perturbed vector field are of major interest.

Differentiating (5), (6) with respect to t, expanding f and g in Taylor series around the point $(a\cos\upsilon,-a\omega\sin\upsilon)$ and equating expressions of like powers of μ to zero we obtain an infinite set of equations:

$$\begin{aligned}
&\ddot{u}_1+\omega^2u_1 = f^0+2\omega M_1\sin\upsilon+(2a\omega N_1-\sigma a)\cos\upsilon \quad ,\\
&\ddot{u}_2+\omega^2u_2 = h+(2\omega M_2+aN_{1,a}M_1+aN_{1,\varphi}N_1+2M_1N_1)\sin\upsilon+ \qquad (7)\\
&\qquad\qquad (2\omega N_2-M_{1,a}M_1-M_{1,\varphi}N_1+a^2N_1^2)\cos\upsilon \quad ,\\
&\cdots\cdots
\end{aligned}$$

where coma denotes partial differentiation and:

$$\begin{aligned}
f^0 &\equiv -f(a\cos\upsilon,-a\omega\sin\upsilon) \quad ,\\
f^1 &\equiv -f_{,x}(a\cos\upsilon,-a\omega\sin\upsilon,\nu t)u_1 -\\
&\quad f_{,\dot{x}}(a\cos\upsilon,-a\omega\sin\upsilon,\nu t)(M_1\cos\upsilon-aN_1\sin\upsilon+u_1)-\\
&\quad \sigma u_1-2M_1\dot{u}_{1,a}-2N_1u_{1,\varphi} \quad ,\\
h &\equiv f^1 \qquad\qquad \text{for (3.a)},\\
h &\equiv f^1+g^0 \qquad \text{for (3.b)}.
\end{aligned}$$

Eqs (7) are linear, with the right sides 2π periodic in νt and υ ($\upsilon=\omega t+\varphi$). We can solve them recursively, expanding the

right sides into Fourier series and making use of linearity. We can remove secular terms in each of eqs (7) requiring that coefficients at $\sin\upsilon$, $\cos\upsilon$ in these expansions be equal to zero. We do this by the appropriate choice of M_i, N_i $(i=1,2...)$.

In practice, functions f,g are often polynomials in $x,\dot{x}$ and have finite number of harmonic functions of νt. Then we do not need to worry about Taylor and Fourier expansions and can confine our calculations only to elementary trigonometry and algebra.

Having determined M_i, $N_i (i=1,2...)$ we get the right sides of (6). We denote them:

$$M(a,\varphi,\nu) \equiv \mu M_1(a,\varphi) + \mu^2 M_2(a,\varphi) + \ldots \quad ,$$
$$N(a,\varphi,\nu) \equiv \mu N_1(a,\varphi) + \mu^2 N_1(a,\varphi) + \ldots \quad .$$

Here we emphasized, that ν is a parameter in these relations.

Thus, we obtain a two-dimensional flow:

$$\begin{aligned} \dot{a} &= M(a,\varphi,\nu) \quad , \\ \dot{\varphi} &= N(a,\varphi,\nu) \quad . \end{aligned} \tag{8}$$

To get stationary solutions of (3.a), (3.b) we require that

$$\begin{aligned} M(a,\varphi,\nu) &= 0 \ , \\ N(a,\varphi,\nu) &= 0 \ . \end{aligned} \tag{9}$$

We denote the solutions of (8) by a_o, φ_o. Stability of these solutions may be investigated in usual way: we consider the disturbed solution:

$$a = a_o + \delta a, \quad \varphi = \varphi_o + \delta\varphi. \tag{10}$$

For the disturbance we obtain from (8) linear equations:

$$(\delta a)^{\cdot} = M_{,a}\delta a + M_{,\varphi}\delta\varphi \ ,$$
$$(\delta\varphi)^{\cdot} = N_{,a}\delta a + N_{,\varphi}\delta\varphi \ , \qquad (11)$$

with the derivatives calculated in (a_o,φ_o).
The characteristic equation for (11) is

$$\lambda^2 + b\lambda + c = 0 \ ,$$

with $b \equiv -(M_{,a} + N_{,\varphi})$, $c \equiv M_{,a}N_{,\varphi} - N_{,a}M_{,\varphi}$.
a_o,φ_o are known to be stable if the Routh-Hurvitz criteria for (11) are satisfied:

$$b \equiv -(M_{,a} + N_{,\varphi}) > 0 \ , \qquad (12.a)$$
$$c \equiv M_{,a}N_{,\varphi} - M_{,\varphi}N_{,a} > 0 \ . \qquad (12.b)$$

Condition (12.a) is fulfilled if (8) is dissipative. If we pass through the stability boundary c=0 from positive to negative values of c one of the eigenvalues (characteristic exponents) λ becomes positive, with both λ remaining real.

We will clarify the meaning of (12.b) in terms of resonance curves $a = a_o(\nu)$ in (a,ν) plane. Differentiating (9) with respect to ν we obtain

$$M_{,a}\frac{da}{d\nu} + M_{,\varphi}\frac{d\varphi}{d\nu} + M_{,\nu} = 0 \ ,$$
$$N_{,a}\frac{da}{d\nu} + N_{,\varphi}\frac{d\varphi}{d\nu} + N_{,\nu} = 0 \ ,$$

and solving for $\frac{da}{d\nu}$:

$$\frac{da}{d\nu} = -(M_{,\nu}N_{,\varphi} - M_{,\varphi}N_{,\nu})/(M_{,a}N_{,\varphi} - M_{,\varphi}N_{,a}) \qquad (13)$$

From (13) and (12.b) we conclude that the points, where $a=a_o(\nu)$ has vertical tangent correspond to stability limits.

Another question we want to raise here is: how the disturbances δa, $\delta\varphi$ influence Fourier spectra of solutions (5)? To answer it, we expand the obtained approximate periodic solution in Fourier series:

$$x(a,\varphi,t) = \sum_{i=0,1,2,3\ldots} [p_i(a,\varphi)\cos i\omega t + q_i(a,\varphi)\sin i\omega t] \qquad (14)$$

and disturb a and φ. If we use (10) and expand p_i, q_i into Taylor series around (a_o, φ_o) we obtain from (14)

$$x(a,\varphi,t) = \sum_{i=0,1,2,3\ldots} [p_i(a_o,\varphi_o)\cos i\omega t + q_i(a_o,\varphi_o)\sin i\omega t] + \sum_{i=0,1,2,3\ldots} [P_i\cos i\omega t + Q_i\sin i\omega t], \qquad (15)$$

where P_i, Q_i denote all terms from Taylor expansion containing derivatives of p_i, q_i calculated in a_o, φ_o and disturbances $\delta a, \delta\varphi$ The first sum in (15) is the solution x(t), the second is the disturbance due to the disturbances δa, $\delta\varphi$ of amplitude and phase. This second term may be denoted:

$$\delta x(t) = \sum_{i=0,1,2,3\ldots} [P_i\cos i\omega t + Q_i\sin i\omega t] .$$

We want to show here that the disturbance $\delta x(t)$ can not include growing in time harmonics with frequencies other then Fourier components of the solution x(t). To prove this, we note that new harmonics can appear in (15) only for complex λ ie in the case $b^2 - 4c < 0$. For dissipative systems (b>0) it requires c>0, but then the solution is stable, due to (12.b), and the disturbances vanish, not grow, exponentially. Thus we conclude that stability analysis based on the perturbation technique does not allow us to investigate instabilities having other frequencies, than these in the Fourier spectrum of the solution itself.

2.2 Fundamental resonances

2.2.1. Introduction

a.) Large Orbit solution

In the near-linear perturbation techniques usually all nonlinear, forcing and damping terms are treated as the

perturbation terms (see [6], [25], also Bogoliubov,Mitropolsky [26], Nayfeh [27] for examples). If we followed exactly this approach we would introduce small parameter μ into (1) as follows:

$$\ddot{x} - \alpha x + \mu(\bar{\beta}x^3 + \bar{h}\dot{x} - \bar{F}\cos\nu t) = 0 \quad , \tag{16}$$

with $\beta=\mu\bar{\beta}$, $h=\mu\bar{h}$, $F=\mu\bar{F}$, $\mu>0$.

Unfortunately (16) is not of the form (2.a), (2.b). It has for $\mu=0$ nonperiodic, exponentially growing solutions and can not be considered a good zeroth approximation of the oscillator (1). Thus we seek a better starting point of the perturbation procedure.

Our approach is a sort of combination between the near-linear and near-Hamiltonian techniques. It consists in what follows:

1. As in near-Hamiltonian methods we consider first a nonlinear Hamiltonian equation, describing free (undamped, unforced) vibrations of the original system. In our case the equation is of the form:

$$\ddot{x} - \alpha x + \beta x^3 = 0. \tag{17}$$

Then we find a harmonic linearization of the Hamiltonian equation. Below we use harmonic balance method, which is known to be equivalent to harmonic linearization.

Assuming $x(t)$ in the form: $x(t)=a\cos\Omega t$ and substituting into (17) we get:

$$-a\Omega^2\cos\Omega t + \beta a^2(3\cos\Omega t + \cos 3\Omega t)/4 - \alpha a\cos\Omega t = 0 \quad .$$

Dropping 3Ω frequency term we can write:

$$\ddot{x} + \Omega^2(a)x = 0, \tag{18}$$

with the "natural frequency" $\Omega^2(a)= - \alpha + 3\beta a^2/4$. Eq (18) is thus a linear system approximating nonlinear eq (17).

2. We consider the original problem as a perturbation of the

linearized equation (18). First we write (1) as:

$$\ddot{x} + \Omega^2(a)x + [-\alpha x + \beta x^3 - \Omega^2(a)x] + h\dot{x} - F\cos\nu t = 0 \ . \qquad (19)$$

Let us suppose that $h=o(\mu)$, $F=o(\mu)$. We can also assume that $(-\alpha + \beta x^2 - \Omega^2(x))x = o(\mu)$, because we approximated $-\alpha x + \beta x^3$ by $\Omega^2(a)x$ in harmonic linearization. Thus we can write (19) as:

$$\ddot{x} + \Omega^2(a)x + \mu[(-\bar{\alpha} + \bar{\beta}x^2 - \bar{\Omega}^2(a)]x + \bar{h}\dot{x} - \bar{F}\cos\nu t = 0 \ , \qquad (20)$$

where $\alpha=\mu\bar{\alpha}$, $\Omega^2=\mu\bar{\Omega}^2$, $\beta=\mu\bar{\beta}$ and $h=\mu\bar{h}$, $F=\mu\bar{F}$.

The system (20) is formally linear for $\mu=0$ because $\Omega^2(a)$ does not depend on x, $\dot{x}$, t. Ω^2 depends, however, on the amplitude a of the fundamental harmonic in the sought solution.

b.) Small Orbit solution

Together with equation (1) we will consider another equation, describing displacement from the stable equilibrium point. The system (1) has three equilibria points: one unstable for $x=0$ and two stable (bottoms of the wells) for $x=\pm\sqrt{\beta/\alpha}$. For the deflection $y=x\mp\sqrt{\beta/\alpha}$ we obtain:

$$\ddot{y}+h\dot{y}+\alpha_1 y+\alpha_2 y^2+\alpha_3 y^3=F\cos\nu t \ , \qquad (21)$$

with $\alpha_1 = 2\alpha$, $\alpha_2 = \mp 3\sqrt{\alpha\beta}$, $\alpha_3 = \beta$.

The frequency of small, undamped free vibrations around the stable equilibrium point is $\sqrt{\alpha_1}$

Throughout this paper we will describe SO motions in terms of the displacement y(t), applying the equation of motion in the form (21), not in the form (1). In (21) we have positive stiffness for the equilibrium point $y=0$ and can assume that linear equation:

$$\ddot{y} + \alpha_1 y = 0 \qquad (22)$$

is a good zeroth approximation of the perturbed problem. We might try to find better starting point of the perturbation procedure, using harmonic linearization, like in the LO case. We do not regard it necessary, as the linearized natural frequency, obtained from eq. (21) at F=0, h=0, equals to:

$$\Omega^2(a) = \alpha_1 + \alpha_2 a/2 + 3\alpha_3 a^2/4$$

and does not differ much from α_1 for Small Orbits (amplitude a small). Thus we retain the zeroth approximation equation in the classic form, generic for near-linear perturbation methods.

The equation (21) has quadratic and cubic nonlinearities. Basing on rescaling properties we put the cubic term of one order in μ higher then the quadratic term. We will also put damping and forcing effects of the same order as the cubic term, knowing that perturbation methods need higher order approximations to capture the effects of quadratic terms. This way we will meet damping and forcing in the second order of perturbation procedure instead of in the first order, obtaining the final solution in simpler form. Therefore we consider an equation of the (2.b) type:

$$\ddot{y} + \alpha_1 y + \mu\bar{\alpha}_2 y^2 + \mu^2(\bar{h}\dot{y} + \bar{\alpha}_3 y^3 - \bar{F}\cos\nu t) = 0 \ , \qquad (23)$$

where $\alpha_2 = \mu\bar{\alpha}_2$, $h = \mu\bar{h}$, $\alpha_3 = \mu^2\bar{\alpha}_3$, $F = \mu^2\bar{F}$.

2.2.2 LO 1:1 resonance

Having prepared for the Large Orbit problem the equation (20) we can start the perturbation procedure. (20) has the form (2.a). For the 1:1 resonance we put m=n=1 , require that $\Omega^2(a) - \nu^2 = \mu\sigma$ (condition (4.a)), and transform (20) to the form corresponding to eq (3.a):

$$\ddot{x} + \nu^2 x + \mu[(\sigma - \bar{\alpha} + \bar{\beta}x^2 - \bar{\Omega}^2(a))x + \bar{h}\dot{x} - \bar{F}\cos\nu t] = 0. \qquad (24)$$

Now we assume the solution in the form containing terms μ^0 and μ^1:

$$x(t) = a\cos(\nu t+\varphi) + \mu x_1(a,\varphi,t). \qquad (25)$$

The perturbation method yields:

$$2\mu D_1 \nu + h\nu a + F\sin\varphi = 0 ,$$

$$a[2\mu E_1 \nu - \Omega^2(a) + \nu^2] + F\cos\varphi = 0 ,$$

and

$$\mu x_1(a,\varphi,t) = \frac{\beta a^3}{32\nu^2}\cos 3(\nu t+\varphi). \qquad (26)$$

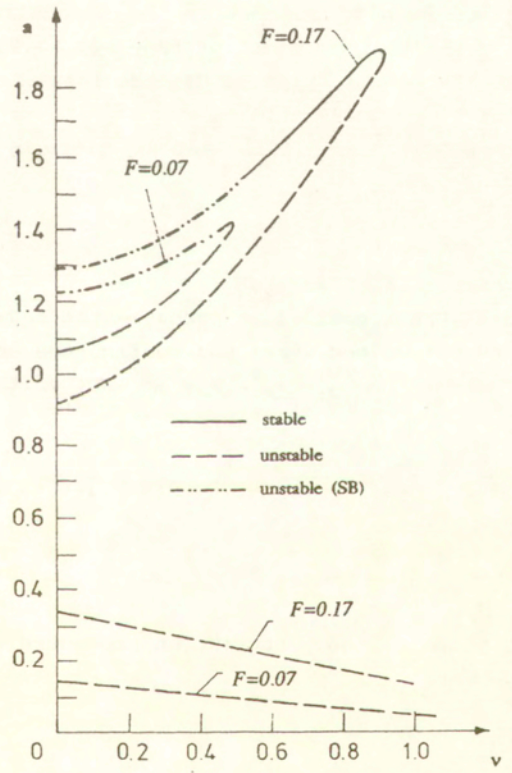

Fig.2. Resonance curves of 1T Large Orbit solution

Taking steady-state conditions (9) into account we get:

$$a = F/\sqrt{(\Omega^2(a) - \nu^2) + (h\nu)^2}\ , \tag{27.a}$$

$$tg\varphi = -h\nu/[\Omega^2(a) - a^2]\ . \tag{27.b}$$

Resonance curves $a(\nu)$ are depicted in Fig 2. The rightmost points correspond to cyclic fold bifurcations creating stable (node) and unstable (saddle) solutions. Left-hand parts of upper branches can become unstable due to symmetry breaking (SB) instability. This instability introduces new frequencies into the solution and is not detected by the inequalities (12). We will use Hill's variational equation (see sec. 3.2) to find it.

Concluding, the sought solution has the form:

$$x(t) = a\cos(\nu t+\varphi) + \mu x_1(a,\varphi,t)\ , \tag{28}$$

with a,φ given by (27.a), (27.b) and μx_1 given by (26).

2.2.3 Small Orbit 1:1 resonance

For the Small Orbit problem we prepared the equation (23). It has the form (2.b). We set m=n=1 and confine our analysis to the region of ν, where $\alpha_1 - \nu^2 = \sigma\mu^2$. Now we can write (23) in the form (3.b):

$$\ddot{y} + \nu^2 y + \mu\bar{\alpha}_2 y^2 + \mu^2(\sigma + \bar{h}\dot{y} + \bar{\alpha}_3 y^3 - \bar{F}\cos\nu t) = 0, \tag{29}$$

and assume

$$y = a\cos(\nu t+\varphi) + \mu y_1(a,\varphi,t) + \mu^2 y_2(a,\varphi,t). \tag{30}$$

In subsequent steps of the perturbation procedure we get:
- from μ^1 equations:

$$M_1 = N_1 = 0\ ,$$

and

$$\mu y_1(a,\varphi,t) = -\frac{\alpha_2 a^2}{2\nu^2} + \frac{\alpha_2 a^2}{6\nu^2}\cos 2(\nu t+\varphi)\ ; \tag{31}$$

- from μ^2 equations:

$$\mu^2 2\nu M_2 + h a\nu + F\sin\varphi = 0 ,$$

$$\mu^2 \nu a N_2 + 5\alpha_2^2 a^3/6 - 3\alpha_3^3/4 - (\alpha_1 - \nu^2)a + F\cos\varphi = 0 ,$$

and the expression for $\mu^2 y_2$ (we will neglect this term).

Steady state conditions (9) take here the form: $M_2 = N_2 = 0$ and yield:

$$a = F/((\Omega^2(a) - \nu^2)^2 + (h\nu)^2), \qquad (32.a)$$

$$tg\varphi = -h\nu/(\Omega^2(a) - \nu^2), \qquad (32.b)$$

where: $\Omega^2(a) \equiv (5\alpha_2^2/6 - 3\alpha_3/4)a^2 + \alpha_1$.

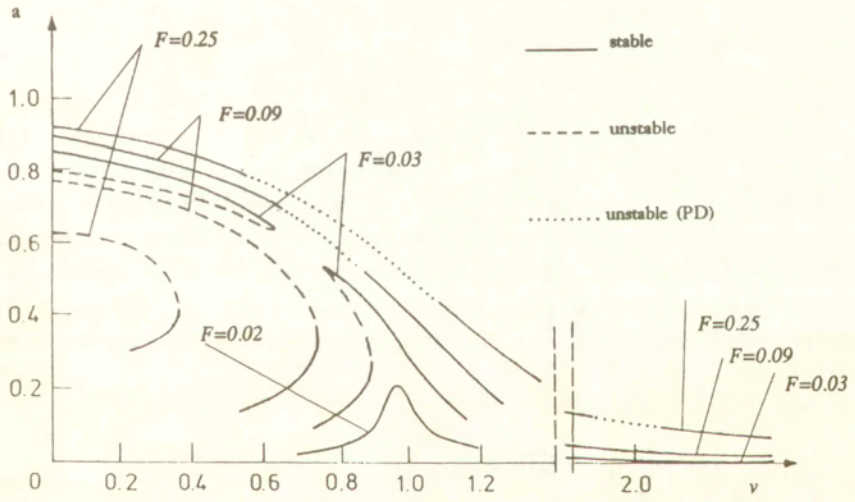

Fig. 3. Resonance curves of 1T Small Orbit solution

Resonance curves $a(\nu)$ for 1:1 SO resonance are shown in Fig 3. For low forces (eg F=0.02) the characteristic looks like for linear oscillator in the region of frequencies close to 1, but

for higher forces (eg F=0.03) two stable solutions (resonant and nonresonant) can coexist with one unstable. A pitchfork bifurcation connects these two situations. For F=0.09 a part of the resonant branch can become unstable due to period doubling instability. The instability appears first in the principal resonance region, but for higher forces (F=0.25) it can affect the solution also in the region of frequencies close to 2. We leave the question of period doubling until sec. 3.3 - this instability can not be found using the conditions 12.

Eventually the solution has the form:

$$y = a\cos(\nu t+\varphi) + \mu y_1(a,\varphi,t) \quad , \tag{33}$$

with a,φ given by (32.a), (32.b) and μy_1 given by (31).

2.3 Subharmonic resonances

2.3.1 Introduction.

As we have seen, the systems of (3.a) type exhibit 1:1 steady-state solutions in the first order approximation of x(t). The resonances 1:m (m>1) for such systems need higher order approximations (see [26] for an example). In order to obtain 1:m subharmonics in lower orders of the perturbation procedure, another approach has been proposed consisting in setting F of order μ^0 instead of order μ^1. Thus, for secondary resonances we write :

- for Large Orbit (19) in the form:

$$\ddot{x} + \Omega^2(a)x + \mu([-\bar{\alpha} + \bar{\beta}x^2 - \bar{\Omega}^2(a)]x + \bar{h}\dot{x}) = F\cos\nu t \quad , \tag{34}$$

instead of the form (20).

- for Small Orbit (21) in the form:

$$\ddot{y} + \alpha_1 y + \mu\bar{\alpha}_2 y^2 + \mu^2(\bar{h}\dot{y} + \bar{\alpha}_3 y^3) = F\cos\nu t \quad , \tag{35}$$

instead of the form (23).

Separate treatment of secondary resonances is a common practice in near-linear perturbation methods ([6],[25-27]). We can not put F of order μ^0 in fundamental resonance analysis, because we would deal then with secular terms problem (arising for $\nu \approx \Omega$) already in the zeroth order equation, where we could not avoid it. Setting $F = o(\mu^1)$ we can move this problem to the first order equation, where it can be solved by the appropriate choice of M_1, N_1. Only when ν is far from Ω, what takes place for secondary resonances, we can set $F = o(\mu^0)$.

Now we transform (28), (29) to the already known form (3.a), (3.b).

-In LO equation (34)
we remove the external forcing term by applying the change of variables:

$$x(t) = z(t) + z_0(t), \qquad z_0(t) = C\cos\nu t,$$

where

$$C = P/(\Omega^2(a) - \nu^2) \ . \tag{36}$$

We obtain for z(t):

$$\ddot{z} + \Omega^2(a)z + \mu[\bar{h}(\dot{z}+\dot{z}_0) + (-\bar{\alpha}-\bar{\Omega}^2)(z+z_0) + \bar{\beta}(z+z_0)^3] = 0. \tag{37}$$

-In SO equation (35)
we apply analogous change of variables

$$y(t) = z(t) + z_0(t), \qquad z_0(t) = C\cos\nu t.$$

Requiring that

$$C = F/(\alpha_1 - \nu^2) \tag{38}$$

we remove the term $F\cos\nu t$ and obtain for z(t):

$$\ddot{z} + \alpha_1 z + \mu\bar{\alpha}_2(z+z_0)^2 + \mu^2[\bar{h}(\dot{z}+\dot{z}_0) + \bar{\alpha}_3(z+z_0)^3] = 0. \tag{39}$$

2.3.2 1:3 Large Orbit resonance

Here n=1,m=3. The detuning relation (4.a) is now:

$\mu\sigma = \Omega^2 - \nu^2/9$

and means that we are in the region of ν close to 3Ω in the parameter space, ie far from the principal resonance. Taking this relation into account we write (37) as:

$$\ddot{z} + (\nu/3)^2 z + \mu[\sigma z + \bar{h}(\dot{z}+\dot{z}_0) + (-\bar{\alpha}-\bar{\Omega}^2)(z+z_0) + \bar{\beta}(z+z_0)^3] = 0 \ . \tag{40}$$

We assume approximate solution in the form:

$$z = a\cos(\nu t/3+\varphi) + \mu z_1(a,\varphi,t) \ . \tag{41}$$

The perturbation method yields:

$$\mu z_1(a,\varphi,t) =$$

$$\frac{9}{8\nu^2}\left(h\nu C\cos 3\varphi + \left[\frac{3}{2}a^2C\beta + \frac{3}{4}\beta C^3 - (\alpha+\Omega^2)C\right]\sin 3\varphi\right)\sin(\nu t+3\varphi) +$$

$$\frac{9}{8\nu^2}\left(h\nu C\sin 3\varphi + \left[\frac{3}{2}a^2C\beta + \frac{3}{4}\beta C^3 - (\alpha+\Omega^2)C\right]\cos 3\varphi + \frac{1}{4}\beta a^3\right)\cos(\nu t+3\varphi) +$$

$$\frac{27}{56\nu^2}\beta Ca^2\cos(\tfrac{5}{3}\nu t+2\varphi) + \frac{27}{56\nu^2}\beta Ca^2\cos(\tfrac{5}{3}\nu t-\varphi) +$$

$$\frac{27}{96\nu^2}\beta Ca^2\cos(\tfrac{7}{3}\nu t+\varphi) + \frac{9}{120\nu^2}\beta C^3\cos 3\nu t \ , \tag{42}$$

and

$$-\frac{2}{3}\mu M_1\nu - \frac{1}{3}h a\nu + \frac{3}{4}\beta Ca^2\sin 3\varphi = 0 \ ,$$

$$-\frac{2}{3}\mu M_1\nu a + [\Omega^2(a) - (\nu/3)^2]a + \frac{3}{2}\beta aC^2 + \frac{3}{4}\beta Ca^2\cos 3\varphi = 0 \ .$$

Steady state conditions (9) take here the form: $M_1 = N_1 = 0$ yielding

$$a = \frac{4}{3\beta C^2}\left(\left[\frac{h\nu}{3}\right]^2 + \left[[\Omega^2(a) - (\nu/3)^2]a + \frac{3}{2}\beta C^2\right]^2\right)^{1/2}, \tag{43.a}$$

$$\mathrm{tg}\,3\varphi = -\left[\frac{h\nu}{3}\right] / \left[\Omega^2(a) - (\nu/3)^2 + \frac{3}{2}\beta C^2\right] \ . \tag{43.b}$$

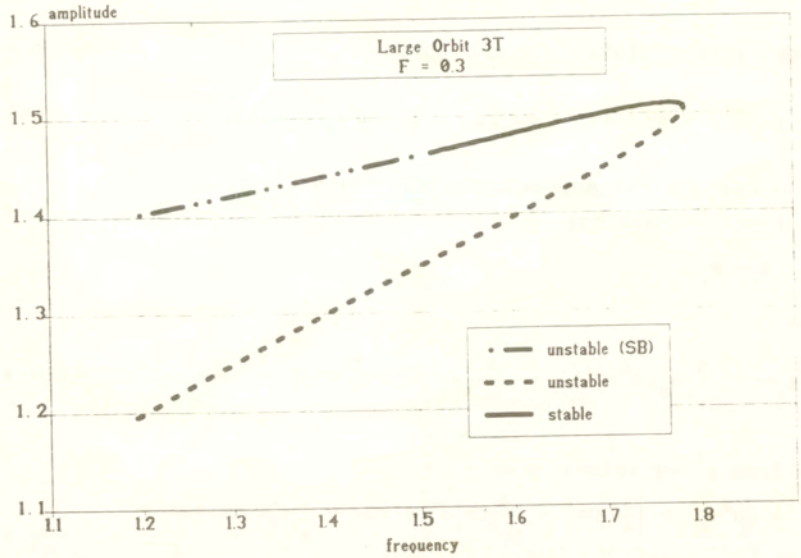

Fig. 4. A resonance curve of 3T Large Orbit solution

A typical resonance curve obtained from the above algebraic equations is shown in Fig.4. The rightmost point corresponds to fold bifurcation creating stable (node) and unstable (saddle) solutions. The left-hand part of the upper branch will be shown unstable due to symmetry breaking instability in sec. 3.2.

Eventually we get for x(t):

$$x(t) = x(t+3T) = C\cos\nu t + a\cos(\nu t/3+\varphi) + \mu z_1(a,\varphi,t), \qquad (44)$$

with C defined by (36), a,φ by (43.a), (43.b) and μz_1 by (42).

2.3.2 1:3 Small Orbit resonance

Here n=1, m=3 and we introduce detuning parameter of the type (10.b): $\mu\sigma^2 = \alpha_1 - \nu^2/9$ and write (39) as

$$\ddot{z} + (\nu/3)^2 z + \mu\bar{\alpha}_2(z+z_0)^2 + \mu^2[\sigma z + \bar{h}(\dot{z}+\dot{z}_0) + \bar{\alpha}_3(z+z_0)^3] = 0. \qquad (45)$$

Seeking the solution in the form:

$$z = a\cos(\nu t/3+\varphi) + \mu z_1(a,\varphi,t) + \mu^2 z_2(a,\varphi,t) \qquad (46)$$

we obtain in the approximate procedure:

- from μ^1 equation:

$$M_1 = N_1 = 0$$

and

$$\mu z_1 = -\frac{9}{2\nu^2}\alpha_2(a^2+C^2) + \frac{3}{2\nu^2}\alpha_2 a^2\cos(\frac{2}{3}\nu t+2\varphi) + \frac{9}{70\nu^2}\alpha_2 C^2\sin 2\nu t \qquad (47)$$

- from μ^2 equation:

$$-\frac{2}{3}\mu^2 M_2\nu + \left[\frac{3}{4}\alpha_3 Ca^2 + \frac{9}{2\nu^2}C\alpha_2^2 a^2\right]\sin 3\varphi + \frac{3}{\nu^2}\alpha_2^2 C^2 a\sin 6\varphi +$$

$$-\frac{ha\nu}{3} = 0 \quad , \qquad (48.a)$$

$$-\frac{2}{3}\mu^2 N_1\nu + \left[\frac{3}{4}\alpha_3 Ca^2 + \frac{9}{2\nu^2}C\alpha_2^2 a^2\right]\cos 3\varphi + \frac{3}{\nu^2}\alpha_2^2 C^2 a\cos 6\varphi +$$

$$-\frac{9}{\nu^2}\alpha_2 a(a^2+C^2) + \frac{3}{2\nu^2}\alpha_2^2 a^2 + \frac{3}{4}\alpha_3 a^3 + \frac{3}{2}\alpha_3 C^2 a + \alpha_1 a +$$

$$-\frac{1}{9}a\nu^2 + \frac{9}{15\nu^2}\alpha_2 C^2 a = 0 \quad , \qquad (48.b)$$

and

the $\mu^2 z_2$ term ,which we neglect.

Setting $M_2 = N_2 = 0$ (this follows from (9) conditions) in the last two equations we get algebraic equations for a and φ. The resonance curve obtained from these equations is depicted in Fig 5. The rightmost point of the curve corresponds to saddle-node bifurcation. The leftmost segment of the upper branch will be shown unstable due to period doubling instability in section 3.3., although it is stable in the sense of the inequalities (12).

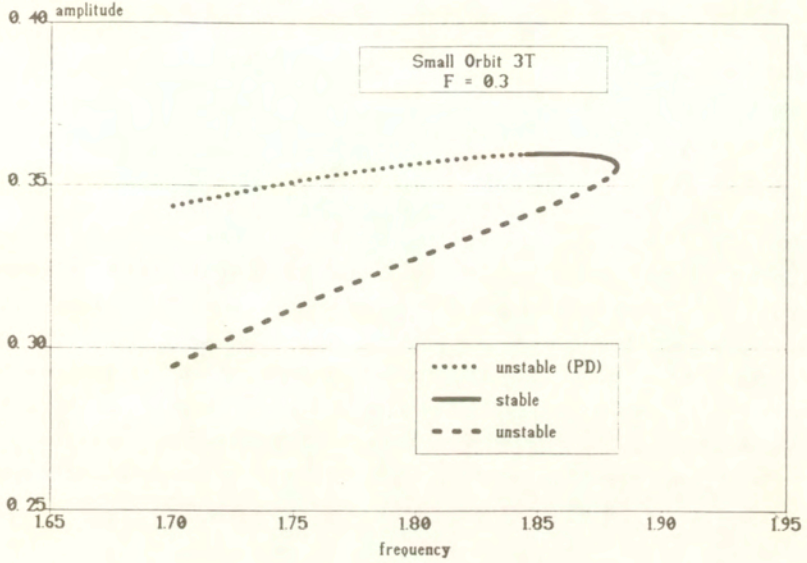

Fig. 5. A resonance curve of 3T Small Orbit solution

As in 1:1 SO resonance case we include in the approximate solution y(t) only μ^0 and μ^1 terms (μ^2 term was used only to determine a and φ) obtaining:

$$y(t) = y(t+3T) = C\cos\nu t + a\cos(\nu t/3+\varphi) + \mu z_1(a,\varphi,t), \quad (49)$$

where C is defined by (38), a,φ by (48.a), (48.b) with $M_2=N_2=0$ and μz_1 by (47).

2.3.3. 1:2 Small Orbit resonance

We could treat this resonance the same way as 1:3 SO case i.e using eq (39), setting n=1 m=2, and assuming the solution :

$$z = a\cos(\nu t/2+\varphi) + \mu z_1(a,\varphi,t) + \mu^2 z_2(a,\varphi,t) \quad (50)$$

with the detuning relation $\alpha_1-\nu^2/4 = \sigma\mu^2$. We leave this form of

solution and detuning relation, but simplify a little the equation. We shift the term $2zz_0$ from μ^1 to μ^2 expression. Thus we rewrite (39) as:

$$\ddot{z} + \alpha_1 z + \mu\alpha_2(z_0^2+z^2) + \mu^2(2\bar{\bar{\alpha}}_2 z z_0 + \bar{h}(\dot{z}_0+\dot{z}) + \bar{\alpha}_3(z_0+z)^3) = 0, \quad (51)$$

where $\mu^2\bar{\bar{\alpha}}_2 = \alpha_2$.
Without this modification we obtain complicated algebraic equations for amplitude and phase of the solution. These equations may be solved only numerically. We want, however, have in this case solution in closed form, which allows further analytical investigations. Despite simplifications we find that we are in satisfactory agreement with experimental results.

The transformation of (2.b) into (3.b) in sec 2.1 corresponds in this case to the transformation of (51) into

$$\ddot{z}+(\nu/2)^2 z+\mu\alpha_2(z_0^2+z^2)+\mu^2[\sigma z + 2\bar{\bar{\alpha}}_2 z z_0 + \bar{h}(\dot{z}_0+\dot{z})+\bar{\alpha}_3(z_0+z)^3]=0. \quad (52)$$

Following the perturbation method we obtain:
- from μ^1 term:

$$M_1 = N_1 = 0$$

and

$$\mu z_1(a,\nu,t) = -\frac{2}{\nu^2}\alpha_2^2 a + \frac{2}{3\nu^2}\alpha_2 a^2\cos(\nu t+2\varphi) \quad (53)$$

- from μ^2 term:

$$-\mu^2 M_2\nu - \frac{1}{2}ah\nu + \alpha_2 aC\sin 2\varphi = 0 ,$$

$$-\mu^2 N_2\nu a - \frac{4}{\nu^2}\alpha_2^2 a(a^2+C^2) + \frac{2}{3\nu^2}\alpha_2^2 a^3 + \frac{3}{4}\alpha_3 a +$$
$$(\frac{3}{2}\alpha_3 C^2 + \alpha_1 - \nu^2)a + \alpha_2 aC\cos 2\varphi = 0 ,$$

and

$\mu^2 z_2$ term, neglected in further computations.

The last pair of equations yields in the stationary case ($M_2 = N_2 = 0$) closed formula for amplitude:

$$a^2(\nu) = (-s \pm \sqrt{p^2-q^2})/r \ , \qquad (54.a)$$

where $p \equiv C\alpha_2$, $q \equiv h\nu/2$, $s \equiv \alpha_1 - \nu^2/4 + 3\alpha_3 C^2/2 - 4\alpha_2^2 C^2/\nu^2$,

$r \equiv -10\alpha_2^2/(3\nu^2) + 3\alpha_3/4$;

and phase:

$$tg2\varphi = \pm q/\sqrt{p^2-q^2} \qquad (54.b)$$

It can be shown analytically, that:

1. The expression c in the formula (13.b) is equal to :

$$c = \pm(2a^2\sqrt{p^2-q^2})/r \ ,$$

where r is negative in the frequencies range considered. Thus the + (-) branch in the formula (54.a) for amplitude is unstable (stable) in the sense of inequality (12.b).

2. In the points where the branches coincide and in the points where $a(\nu)=0$, the curve $a(\nu)$ has vertical tangent.

Resonance curves are depicted in Figures 6.a,b,c,d. Unstable solutions created in fold bifurcations are marked with dashed line. The period doubling instability is marked on the upper branch with dotted line. This form of instability is not detected by condition (12.b) and was found using equations from sec. 3.2.

For small forcing (case a) the rightmost point of $a(\nu)$ corresponds to fold bifurcation. For increasing forces this point lowers and then touches the ν axis. In a narrow range of parameters two points with $a(\nu)=0$ coexist with the fold (case b). For larger forces fold is no longer possible and only two points with $a(\nu)=0$ remain (case c). After some critical value only the upper branch (-) of the solution exists and only one point of intersection with the ν axis is possible (case d).

Neglecting μ^2 term in (38) we obtain eventually the sought 2T-periodic solution:

$$y(t) = y(t+2T) = C\cos\nu t + a\cos(\nu t/2+\varphi) + \mu z_1(a,\varphi,t) \ , \qquad (55)$$

with C given by (38), a,φ by (54.a), (54.b) and μz_1 by (53).

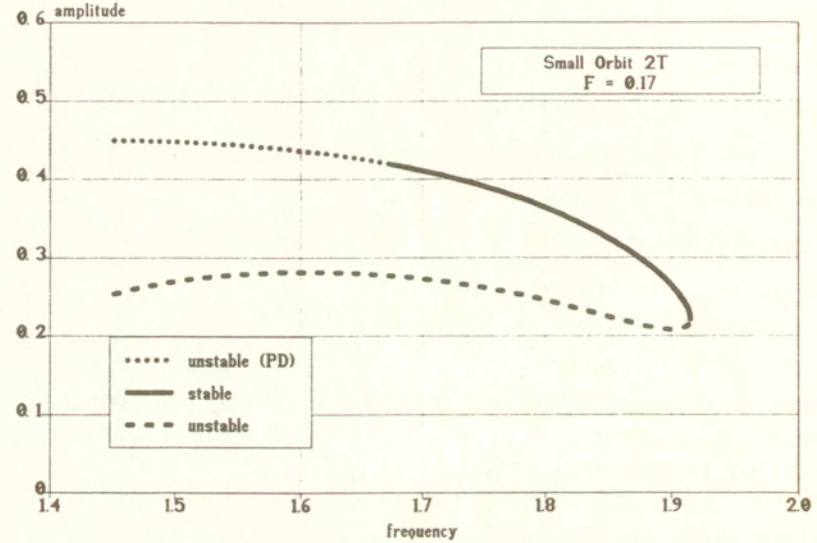

Fig. 6.a

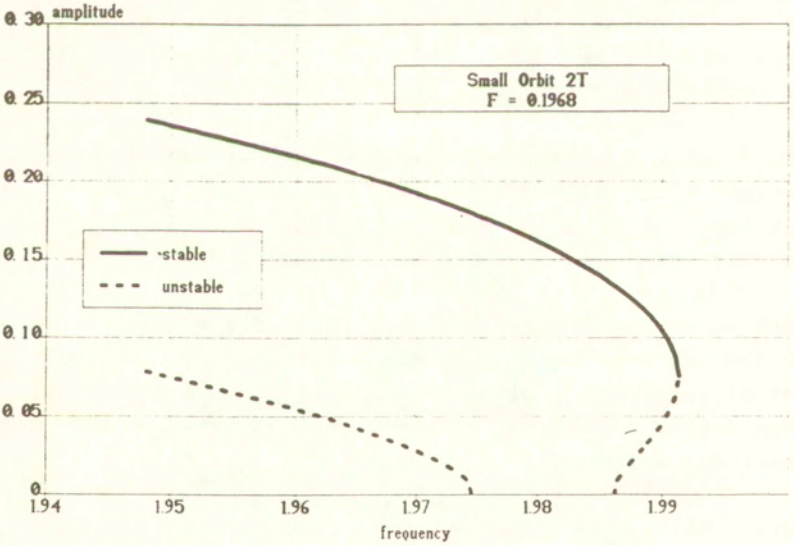

Fig. 6.b

Fig. 6. Resonance curves of 2T Small Orbit solution

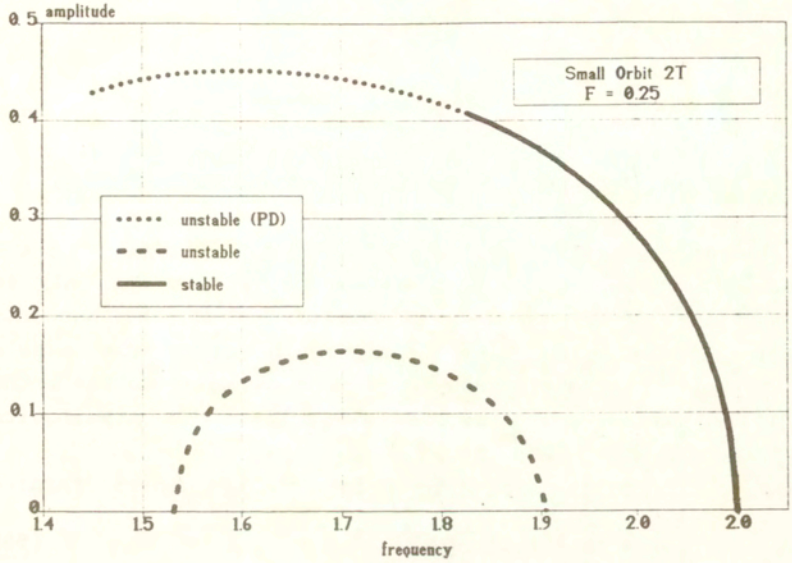

Fig. 6.c

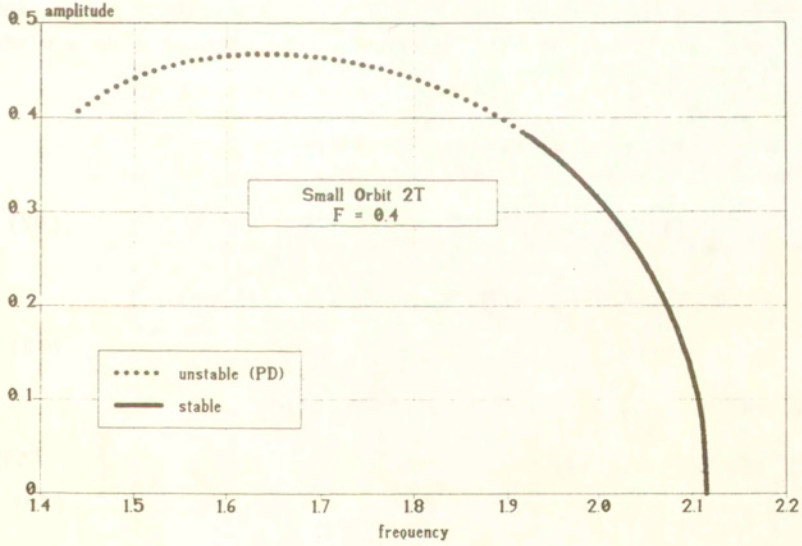

Fig. 6.d

3. Stability analysis and Hill's variational equation

3.1 General theory

As we have seen (sec. 2.1) we can capture so far only the instabilities which consist in the growth of the harmonics already present in the solution. In order to examine instabilities introducing new frequencies we will use the method of Hill's variational equation (see Bolotin [28], Meirovitch [29], Hayashi [30], also [25]).

Having the nonlinear equation written in the general form:

$$\ddot{x} + h\dot{x} + P(x) = G(t) \tag{56}$$

and its (approximate) periodic solution x(t), we disturb this solution by adding $\delta x(t)$ to x(t) and substitute $x+\delta x$ into (42). We will consider x(t) asymptotically stable if $\delta x \to 0$ when $t \to \infty$.

In the linear approximation we get for δx:

$$(\delta x)^{\cdot\cdot} + h(\delta x)^{\cdot} + \frac{\partial P}{\partial x}\Big|_{x(t)}(\delta x) = 0 \tag{57}$$

The change of variables

$$\delta x(t) = \eta(t)e^{-ht/2} , \tag{58}$$

applied to (43), results in Hill's equation:

$$\ddot{\eta} + \gamma(t)\eta = 0 \tag{59}$$

with $$\gamma(t) = \frac{\partial P}{\partial x}\Big|_{x(t)} - h^2/4 \tag{60}$$

We denote the (minimal) period of γ by τ. It may differ from the period of the solution x(t) as we show later.

General results concerning (59) we are interested in come from Floquet theory and are as follows:

i). Any solution of (59) is a linear combination of two independent functions $\theta_1(t)$, $\theta_2(t)$. The functions $\theta_1(t)$, $\theta_2(t)$ may be choosen to satisfy the condition:

$$\theta_1(t+\tau) = \rho_1\theta_1(t) \ , \qquad \theta_2(t+\tau) = \rho_2\theta_2(t),$$

where ρ_1, ρ_2, known as Floquet multipliers, can be obtained from the characteristic equation

$$\rho^2 - 2K\rho + 1 = 0 \ , \tag{61}$$

with $K = [\theta_1(\tau) + \theta_2'(\tau)]/2$.

ii). Three cases are possible:

a) $|K| > 1$

θ_k has the form:

$$\theta_k(t) = \Xi(t)e^{t(\ln|\rho_k|+i\arg\rho_k)/\tau} \ , \tag{62}$$

where $k=1,2$ and $\Xi(t)$ is a τ-periodic function.

Denoting:

$$\Phi_k(t) \equiv \Xi(t)e^{t/\tau i\arg\rho_k} \ ,$$

we can write (62) as:

$$\theta_k(t) = e^{\ln|\rho_k|t/\tau}\Phi_k(t) \ . \tag{63}$$

For $|K|>1$ the roots of (61) are real $\rho_1 = 1/\rho_2$, $|\rho_1|>|\rho_2|$ and θ_1 grows exponentially in time, θ_2 tends to zero. Below we focus on the unbounded (unstable) solutions. We have two possibilities:

1) ρ_k are both real negative. Then

$$\Phi_k(t) = -\Phi_k(t+\tau) = \Phi_k(t+2\tau). \tag{64}$$

From (63) and (64) follows that the growing function θ_1 has representation:

$$\eta_1 \equiv \theta_1 = e^{\varepsilon t} \sum_{n=1,3,5\ldots} [\eta_n^c \cos(n\Pi t/\tau) + \eta_n^s \sin(n\Pi t/\tau)] , \qquad (65)$$

where we denoted

$$\varepsilon \equiv \ln|\rho_1|/\tau \qquad (\varepsilon \text{ real, positive}) \qquad (66)$$

Note, that η_1 has twice the period of the function γ in (59).

2) ρ_k are both real positive. Then

$$\Phi_k(t) = \Phi_k(t+\tau) . \qquad (67)$$

From (63), (66), (67) follows that we can express θ_1 as:

$$\eta_2 \equiv \theta_1 = e^{\varepsilon t} \sum_{n=0,2,4\ldots} [\eta_n^c \cos(n\Pi t/\tau) + \eta_n^s \sin(n\Pi t/\tau)] \qquad (68)$$

In this case η_2 is the solution of (59), which has the same period as $\gamma(t)$. Eqs (65), (68) represent two different forms of unbounded (unstable) solutions.

b) $|K| < 1$

Then the roots of (61) are complex conjugate $|\rho_1| = |\rho_2| = 1$. The solutions θ_k have also the form (62), both being bounded and, generally, quasiperiodic.

c) $|K| = 1$

θ_k have the form:

$\theta_1(t) = \Xi_1(t)$, $\theta_2(t) = \Xi_2(t) + t\Xi_3(t)$,

where Ξ_1, Ξ_2, Ξ_3 are periodic functions of t.

The case c) is the stability boundary for (59). We are, however, interested in the behavior of δx. Looking at (58) we can allow exponential growth of $\eta(t)$, not faster than $e^{ht/2}$. Therefore we will consider the case a). The stability boundary condition may be expressed as

$$\varepsilon = h/2. \qquad (69)$$

iii.)

We recall also some properties of the Hill's equation of the type:

$$\ddot{\eta} + [\Omega_0^2 + \mu\bar{\gamma}(t)]\eta = 0 \quad , \tag{70}$$

with $\bar{\gamma}(t)$ τ-periodic; $\bar{\nu}=2\Pi/\tau$; Ω_0=const; $\mu,\bar{\nu}$-parameters; which we will need later. Eq (70) is a parametric perturbation of the simple linear oscillator and is known to possess in $(\bar{\nu},\mu)$ space regions with unbounded solutions. The regions touch $\bar{\nu}$ axis and widen with increasing parametric excitation μ. Unbounded solutions in the regions are of the form:

η_1 for the regions emanating from the points

$$\bar{\nu}=2\Omega_0/k \quad , \; k=1,3,5\ldots \; , \tag{71.a}$$

η_2 for the regions emanating from the points

$$\bar{\nu}=2\Omega_0/k \quad , \; k=2,4,6\ldots \; . \tag{71.b}$$

Now we take advantage from the results described in i)-iii) in order to determine stability properties of δx. Due to periodicity of (59) we can expand γ into Fourier series. Fundamental solutions in the neighbourhood of stability boundary are already expressed by trigonometric series (65), (68). Therefore we can use the harmonic balance method: on expanding $\gamma(t)$ into Fourier series, we substitute (65) or (68) to (59). Equating coefficients at $\cos(n\Pi t/\tau)$, $\sin(n\Pi t/\tau)$ to zero we obtain an infinite homogeneous set of linear equations for η_n^s, η_n^c. The necessary and sufficient condition for nonzero η_1 (η_2) solutions of (59) is that the determinant of this set be equal to zero. We denote the above condition as:

$$\Delta(\varepsilon^2) = 0 \; . \tag{72}$$

On the stability boundary the condition (69) must be satisfied. Thus we obtain the algebraic equation:

$$\Delta(h^2/4) = 0 \; , \tag{73.a}$$

which must be obeyed by parameters of the system (59) on the stability limit.

To determine stable and unstable regions of parameters we expand (72) in Taylor series around $\varepsilon^2=h^2/4$:

$$\Delta(h^2/4) + \frac{\partial\Delta}{\partial\varepsilon^2}\Big|_{\varepsilon^2=h^2/4}(\varepsilon^2-h^2/4) = 0 \ .$$

In unstable regions $\varepsilon^2>h^2/4$ hence

$\Delta(h^2/4)$ and $\frac{\partial\Delta}{\partial\varepsilon^2}\Big|_{\varepsilon^2=h^2/4}$ must have opposite signes. (73.b)

Concluding, we can use (73.a) as stability limit condition and then use (73.b) to examine on which side of this limit the solutions are unstable.

We emphasize here, that in this paper we use finite Fourier representations for $\gamma(t)$ and seek η_1,η_2 as finite series. Therefore the determinant Δ is also finite. The order of truncation of the series (65), (68) is related to the properties described in the point iii) in the following way:

Suppose that we retained N terms in the sum η_1 or η_2. ([25], [29], [30]). We obtain N regions corresponding to unbounded solutions for each form η_1, η_2. The regions emanate from the points given by (71.a,b). Including new term into the assumed solution we:

- obtain new region in the parameter space,
- correct the shape of the regions obtained in preceding approximations.

For example:

Let us assume that our Hill's equation has the form (70) with $\Omega_0 \approx 1$ and we are interested in unbounded solutions having twice the period of the function $\bar{\gamma}$ in the frequencies region close to $\bar{\nu}=2$. Taking the solution η_1 and setting k=1 in the first order approximation (eqs 71) we obtain the first region corresponding to unbounded solutions. If we are interested in unbounded solutions of η_1 type for lower frequencies we should take k=1,3. Then a new region occurs in the neighbourhood of $\bar{\nu}=2/3$ in the

parameter space. The former region obtained in k=1 approximation is now slightly corrected.

3.2 Symmetry Breaking (SB) instability

We call a $\bar{T}$ periodic orbit symmetric if

$$x(t+\bar{T}/2) = -x(t). \tag{74}$$

Thus the phase portrait (x,x) of an symmetric orbit has a center of symmetry in (0,0). The relation (74) may be satisfied if and only if the Fourier spectrum of x(t) has only odd harmonics with frequencies $2\Pi n/\bar{T}$ (n=1,3,5...). It may be shown (Räty, von Boehm, Isomäki [31]) that in Duffing system only odd subharmonics may be symmetric ie $\bar{T}=kT$ (k=1,3,5...), where T is the driving force period.

If for certain parameter changes the solution ceases to obey the condition (74) we call it symmetry breaking bifurcation. Obviously, even harmonics occur then in the Fourier spectrum of the new orbit.

In this section we are interested in symmetry breaking instability ie in the build-up of even harmonics in the disturbance $\delta x(t)$ of the symmetric solution. Physically,such instability means that we can no longer observe symmetric solution in experiment. Which solution is stable after the instability is a question of further investigation.

Note, that both solutions 1:1 LO and 1:3 LO (eqs (28), (44)) may be generally written as:

$$x(\zeta(t)) = \sum_{i=1,\ 3,5..} [p_i \cos i\zeta + q_i \sin i\zeta] , \tag{75}$$

where $p_i=p_i(a,\varphi,\nu,F)$, $q_i=q_i(a,\varphi,\nu,F)$ and

$\zeta=\nu t$ i=1,3 in 1:1 LO case,

$\zeta=\nu t/3$ i=1,3,5,7,9 in 1:3 LO case.

Thus x(t) are symmetric and $x(\zeta)=-x(\zeta+\pi)$. In our case, for x given by (75) and $\frac{\partial P}{\partial x}=-\alpha+3\beta x^2$, the Hill's equation has the form (70) with:

$$\Omega_0^2 = -h^2/4 + \lambda_0 \quad , \tag{76.a}$$

$$\mu\bar{\gamma} = \sum_{i=2,4,6\ldots} [\lambda_i^c \cos i\zeta + \lambda_i^s \sin i\zeta] \quad , \tag{76.b}$$

where λ_0, λ_i^c, λ_i^s are known function of p_1, q_1. Here $\bar{\gamma}(t)$ is $mT/2$ periodic in t for 1:m resonances (m=1,3). Thus the period of $\bar{\gamma}$ is half the period of the subharmonic solution x(t).

From eq (68) we conclude, that the form η_2 yields disturbances corresponding to symmetry breaking instability. We use the following approximate form of (68):

$$\eta(t) = e^{\varepsilon t}(\eta_0 + \eta_2^c \cos 2\zeta + \eta_2^s \sin 2\zeta) \quad , \tag{77}$$

(ε real, positive).

For the solution (75) the determinant in the condition (72) takes the form:

$$\Delta_m(a,\varphi,\nu,F,\varepsilon^2) \equiv$$

$$\begin{vmatrix} \lambda + \varepsilon^2 - \frac{h^2}{4} & \frac{\lambda_c^2}{2} & 0 \\ \frac{\lambda_c^2}{2} & -4\left(\frac{\nu}{m}\right)^2 + \lambda_0 + \varepsilon^2 - \frac{h^2}{4} + \frac{\lambda_4^c}{2} & 4\nu\varepsilon \\ 0 & -4\nu\varepsilon & -4\left(\frac{\nu}{m}\right)^2 + \lambda_0 + \varepsilon^2 - \frac{h^2}{4} - \frac{\lambda_4^c}{2} \end{vmatrix}$$

where m=1 or m=3 correspond to 1:m LO resonances, hence we can rewrite this condition as:

$$\Delta_m(a,\varphi,\nu,F,\varepsilon^2)=0 \qquad m=1,3.$$

The equation (73.a) must be satisfied on the stability boundary:

$$\Delta_m(a,\varphi,\nu,F,h^2/4)=0.$$

The determinant $\Delta_m(a,\varphi,\nu,F,h^2/4)$ is then a function of ν via $a(\nu)$, $\varphi(\nu)$ (F=const, h=const). The condition (73.b) may be examined by calculating this determinant and its derivative along resonance curves. In Figs 2 and 4 we separated this way stable and unstable fragments of the upper branch.

3.3 Period doubling (PD) instability

Period doubling instability manifests itself by a build-up of the harmonic components, which have period equal to 2mT, where mT is the period of the solution considered (m is the number of resonance). Thus we may expect, that the disturbance $\delta x(t)$ includes component with the frequency $\nu/(2m)$ and its multiples.

First we note, that Small Orbit 1:1, 1:2, 1:3 solutions (eqs.33,49,55) may be written as:

$$x(\zeta(t)) = \sum_{i=0,1,2,3\ldots} [p_i \cos i\zeta + q_i \sin i\zeta] \ , \qquad (78)$$

where $p_i=p_i(a,\varphi,\nu,F)$, $q_i=q_i(a,\varphi,\nu,F)$ and

$\zeta=\nu t$ $\quad i = 0,1,2$ in the 1:1 SO case,

$\zeta=\nu t/2$ $\quad i = 0,1,2$ in the 1:2 SO case,

$\zeta=\nu t/3$ $\quad i = 0,1,2,6$ in the 1:3 SO case.

Here $\frac{\partial P}{\partial x}=\alpha_1+2\alpha_2 x+3\alpha_3 x^2$ and $x(t)$ is given by (78). Thus we obtain the Hill's equation (70) with:

$$\Omega_0^2 = -h^2/4 + \lambda_0 \ , \qquad (79.a)$$

$$\mu\bar{\gamma} = \sum_{i=1,2,3\ldots} [\lambda_i^c \cos i\zeta + \lambda_i^s \sin i\zeta] \ , \qquad (79.b)$$

where $\lambda_0, \lambda_1^c, \lambda_1^s$ functions of p_1, q_1 and λ_1^c, λ_1^s do not vanish simultaneously. It follows that $\bar{\gamma}(t)$ is mT periodic in 1:m resonances (m=1,2,3) ie has the same period as the corresponding subharmonic solutions. Here the instability forms of η_1 type have twice the period of the solution x(t) - see eq (65).

We seek the instability in the form including two terms of the expansion (65):

$$\eta(t) = e^{\varepsilon t}(\eta_{1/2}^c \cos\zeta/2 + \eta_{1/2}^s \sin\zeta/2 + \eta_{3/2}^c \cos 3\zeta/2 + \eta_{3/2}^s \sin 3\zeta/2) \quad , \tag{80}$$

with ε real, positive.

Denoting

$$\Delta_m(a,\varphi,\nu,F,\varepsilon^2) \equiv$$

$$\begin{vmatrix} \varepsilon^2 - \frac{h^2}{4} - \left(\frac{\nu}{2m}\right)^2 + \frac{\lambda_1^c}{2} & \frac{\varepsilon\nu}{m} + \frac{\lambda_1^s}{2} & \frac{\lambda_1^c+\lambda_2^c}{2} & \frac{\lambda_1^s+\lambda_2^s}{2} \\ -\frac{\varepsilon\nu}{m} + \frac{\lambda_1^s}{2} & \varepsilon^2 - \frac{h^2}{4} - \left(\frac{\nu}{2m}\right)^2 - \frac{\lambda_1^c}{2} & \frac{\lambda_2^s-\lambda_1^s}{2} & \frac{\lambda_1^c+\lambda_2^c}{2} \\ \frac{\lambda_1^c+\lambda_2^c}{2} & \frac{\lambda_2^s-\lambda_1^s}{2} & \varepsilon^2 - \frac{h^2}{4} - \left(\frac{3\nu}{2m}\right)^2 + \frac{\lambda_3^c}{2} & \frac{3\varepsilon\nu}{m} + \frac{\lambda_3^s}{2} \\ \frac{\lambda_1^s+\lambda_2^s}{2} & \frac{\lambda_1^c-\lambda_2^c}{2} & -\frac{3\varepsilon\nu}{m} + \frac{\lambda_3^s}{2} & \varepsilon^2 - \frac{h^2}{4} - \left(\frac{3\nu}{2m}\right)^2 - \frac{\lambda_3^c}{2} \end{vmatrix}$$

where m=1,2,3 correspond to 1:m SO resonances,
we can write the condition (72) as

$$\Delta_m(a,\varphi,\nu,F,\varepsilon^2)=0 \quad .$$

Finally, the conditions (73 a,b) allow us to find stability limits and eliminate unstable parts of the solutions $a(\nu)$, $\varphi(\nu)$. The results of the procedure were depicted in Figs 3,5,6 , where the dotted lines correspond to unstable parts of resonance curves.

3.4 Remark

We have already considered stability problems in section 2.3

obtaining the condition connecting stability limits with vertical tangents on resonance curves. The question arises whether we can obtain this condition using Hill's equation technique. The answer is known positive if we:
- solve nonlinear equation using harmonic balance method
- solve Hill's equation following from this solution also using harmonic balance (with the assumed instability form of the same type as the solution itself) - cf [25], Hayashi [30].

4.2 Analysis of results

4.1 Bifurcations in (ν,F) parameter space. Theoretical and experimental results.

4.1.1 Experimental vs theoretical results.

Experimental bifurcational diagrams and domains of existence of stable subharmonics are depicted in Fig 7. Here we included the region of frequencies considered in [20]. The Melnikov homoclinic function has been also drawn in the figure. In order to compare the computer simulations with the theoretical results the regions, where stable subharmonics 1T SO, 3T LO, 2T SO, 3T SO exist, are depicted separately in the subsequent Figs 8-11. For similar comparisons in the cases of 1:1 LO and 1:1 SO in the principal resonance region see Figs 10 and 12 in [20].

In Fig 8 the region of existence of 1T SO is bounded from above by period doubling. This bifurcation can be either supercritical, creating another attractor with period 2T, or subcritical, causing jump to other types of attractors. In Fig 9 symmetric 3T Large Orbit is bounded from the right by cyclic fold and from the left by symmetry breaking. The SB bifurcation creates an unsymmetric attractor, which is not the object of our theoretical study, but is observed in experiment (cf Fig 7). In Fig 10 2T SO attractor is created in fold (for lower excitations) or in period doubling (for higher forces) and

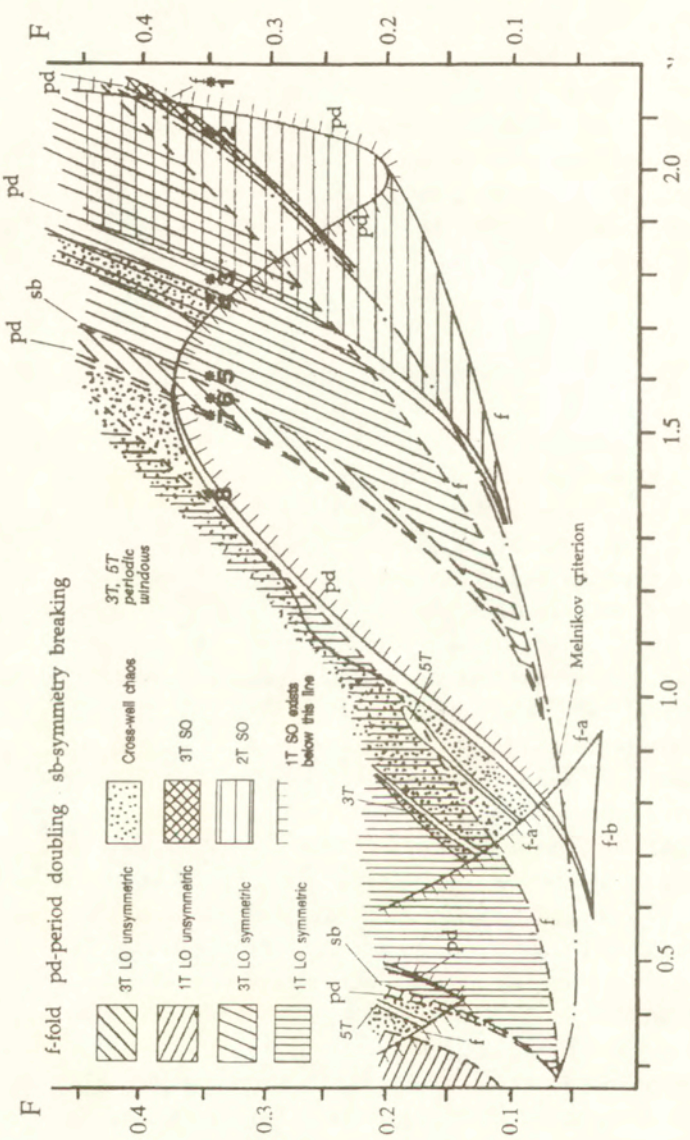

Fig. 7. Regions of existence of various attractors

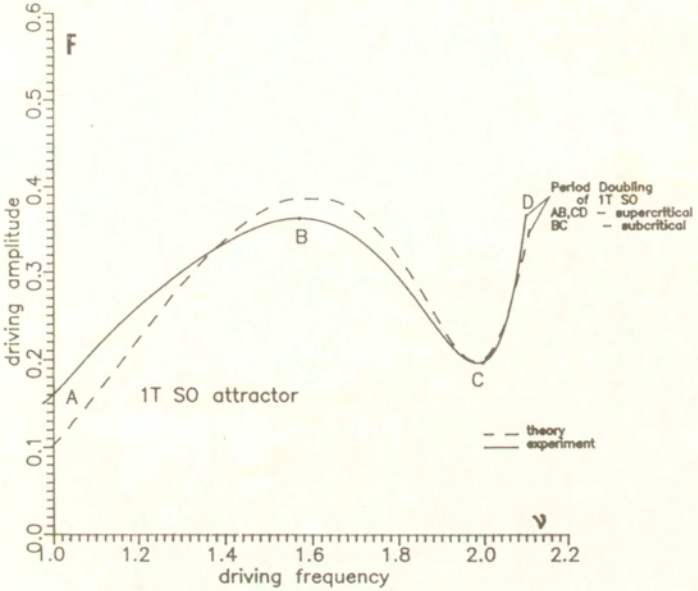

Fig. 8. Region of 1T Small Orbit attractor

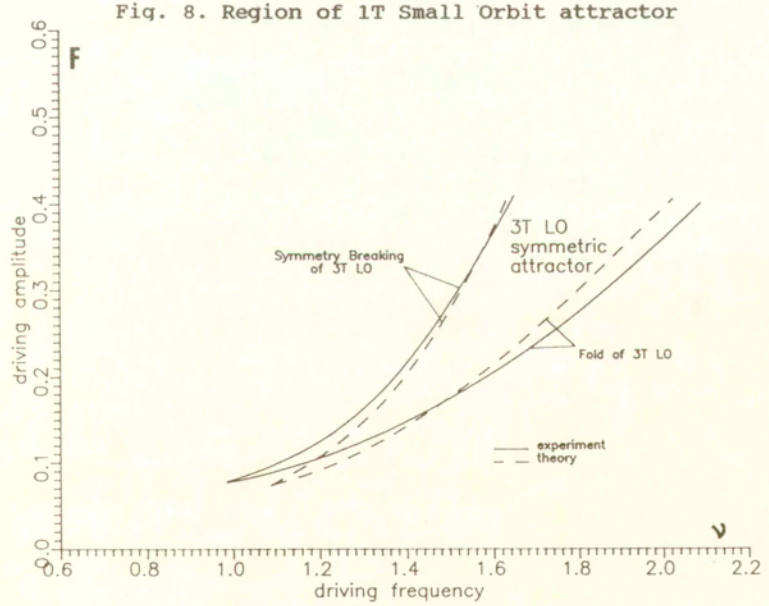

Fig. 9. Region of 3T Large Orbit attractor

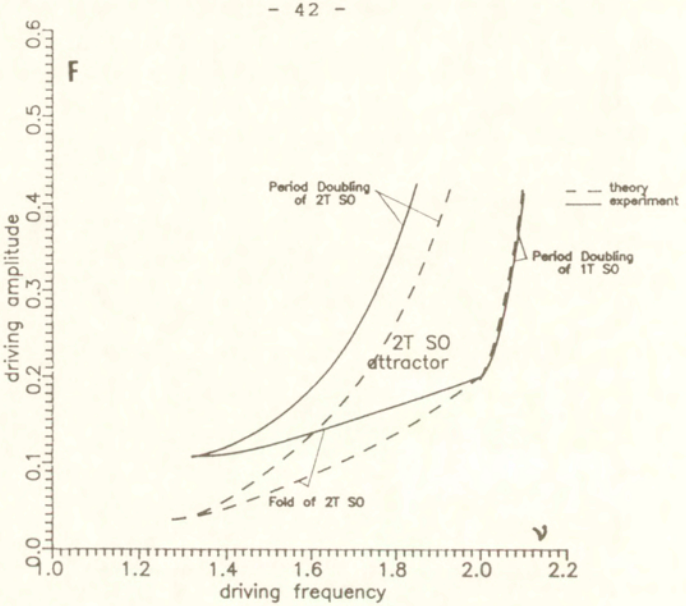

Fig. 10. Region of 2T Small Orbit attractor

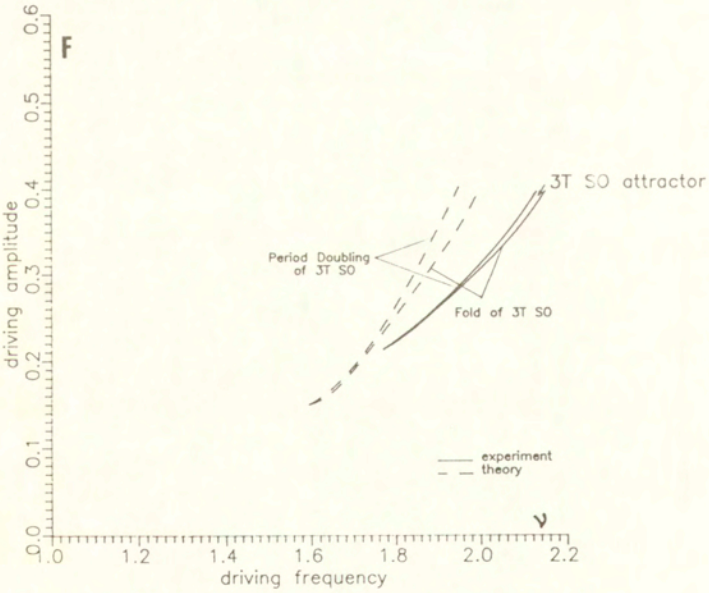

Fig. 11. Region of 3T Small Orbit attractor

destroyed (for decreasing frequencies) in period doubling cascade. In Fig 11 Small Orbit 3T attractor is bounded by fold from the right and by period doubling from the left.

Below we submit a short discussion of the bifurcations responsible for the existence of the subharmonics.

a. Cyclic fold (saddle-node) bifurcations
appear already on amplitude characteristics (figs 2-6) as the points, where $\nu(a)$ has extremal value. Stability of the two branches appearing in each fold can be examined using the conditions (12). This way we can distinguish between unstable (saddle) and stable (node) branches. For all resonances except 1:1 SO we have found one bifurcation of fold type in both experiment and theory. For 1:1 SO, however, two folds are possible in some region of parameters (Fig.7), one creating stable resonant (f-b) the other stable nonresonant solution (f-a) - cf also Fig 3. Moreover, the fold (f-a) is responsible in some parameter range for the creation (destruction) of the chaotic attractor. This differs from the results of Melnikov theory, where only one fold appears in the point (ν=1, F=0) and only one (resonant) orbit is possible (cf Fig 4.6.3 in [6]).

Standard Melnikov theory deals with all subharmonics of mT (m=1,2,3...) type. It predicts that the curves describing fold bifurcations accumulate for fixed ν and $m \to \infty$ on the Melnikov homoclinic function, which for our problem has the form:

$$F(\nu) = \frac{\sqrt{2}h}{3\pi\nu} \cosh(\pi\nu/\sqrt{2}) \qquad (81)$$

and that all LO bifurcation curves lie above and all SO bifurcation curves beneath the curve (81) in the parameter space. It agrees very well with our experiment (see Fig 7). In contrast to Melnikov approach the near-linear method can not capture high order resonances in low order approximations.

b. Period doubling bifurcations
In sec.3.3 we investigated theoretically period doubling

instabilities, leaving the question which solutions are stable after this instability. In all cases we can answer this question using numerical experiment, although in some cases we could help ourselves with some theory:

In sec 2 and 3 we have found

i) 1T SO solution and period doubling instability on this solution (Figs 3,8)

ii) 2T SO solution and points on this solution where $a(\nu)=0$. Moreover, in these points the resonance curve has vertical tangent, possessing the characteristic shape for the amplitude of 2T harmonic born in period doubling - Figs 6,11

We would be happy to prove that the instability of 1T appears exactly when the amplitude of 2T harmonic starts to grow from zero, ie the events i) and ii) take place in the same points of the parameter space. Unfortunately i) and ii) are described by different approximate solutions and we can not expect identity of the corresponding points. We were, however, able to prove that the points are μ-close in the following sense:

- Correcting 1T and 2T solutions by expressions of order μ
- using one-frequency approximation of the assumed form of instability

we can obtain exactly the same points for i) and ii) events. Thus we can see that for low forcings (Figs 6.a,b) stable 1T SO solution is created in cyclic fold bifurcation and for larger forces stable 2T SO appears in period doubling (Figs 6.c,d) of 1T (where the accompanying lost of stability of 1T has been proved with μ-accuracy). This is more then the Melnikov theory states, where only the fold scenario has been described.

Looking at Figs 6. we can classify period doublings corresponding to the points, where the unstable (stable) branch of solution intersects ν axis as subcritical (supercritical). (Cf segments AB, BC and CD in Fig. 8). The subcritical period doubling is responsible in a small range of parameters for the creation (destruction) of the chaotic attractor - cf Fig 14.

2T solutions created in the above scenario appear close to $\nu=2$ and persist in wide parameter range. We associate them

with 1:2 resonance phenomena .

An attempt to describe period doubling in near-Hamiltonian approach has been presented in McRobie,Thompson [21] for similar, one-well potential, "escape equation". The results give good estimates for bifurcations of higher order subharmonics but are less useful in the case of period doublings of 1T orbit. In the latter case Melnikov-like analysis is confined only to the region of frequencies lower then the linear natural frequency of SO motions. Thus the period doublings creating the 1:2 resonance solution do not appear in their paper.

Other period doublings observed in the investigated region are soon followed by other period doublings (being simply beginnings of period doubling cascades). They are all supercritical. It concerns ia the segment AB in Fig 8 and period doublings in Figs 10, 11 as well as the bifurcations, for which we lack theory in the present paper, like period doublings of unsymmetric LO solutions (cf Fig 7).

c. Symmetry breaking bifurcations

We have investigated theoretically only symmetry breaking instabilities without examining what happens after this instability. The simulations indicate that in all considered cases new unsymmetric solutions are born from symmetric ones. Theoretical and experimental symmetry bifurcation curves may be compared in Fig 9 for 1:3 LO and in the ref.[20] in Fig 10 for 1:1 LO resonances.

It has been proved using Poincare maps properties (Swift, Wiesenfeld [32]) that period doublings of symmetric orbits are not possible for Duffing system and that lost of symmetry must precede the period doubling bifurcation. It agrees with our experimental results (Fig 7) and is reflected by the above theory: we notice that Hill's equation obtained from the symmetric solution (with the parametric excitation $\bar{\gamma}(t)$ in the form (76.b)) can not yield period doubling. If we constructed unsymmetric LO solutions we would have Hill's equation with $\bar{\gamma}(t)$ in the form (79.b) allowing period doubling.

4.1.2 Phase portraits of attractors

Here various attractors in (ν,F) space ,corresponding to points 1-8 in Fig.7, are presented. For F=const=0.35 we can observe all major attractor types, which are of interest in the investigated parameter domain. In Fig 12 we illustrate the coexisting attractors using projections of trajectories onto (x,x) plane for periodic and Poincare maps for chaotic motions. Some of the motions are displayed in detail in Fig 13, where we can see the following characteristics for each orbit:

- time history x(t),
- projection onto (x,x) plane,
- Poincare cross-section of the motion taken for t=nT, T - the driving force period, n=1,2,3...
- Fourier spectrum of x(t).

From the symmetry of the system follows that all periodic attractors shown in Fig 12 must appear in pairs [1].

In the point 1 (Fig 13.a) 1T SO attractor is observed. For lower frequencies it undergoes period doubling, creating 2T SO (point 2, Fig 13.b). We have choosen the point 2 as to show the coexisting 3T SO orbit, depicted in detail in Fig 13.c. The 2T orbit bifurcates to 4T (point 3,Fig 13.d). In the point 3. we observe also the symmetric 3T LO orbit, created earlier in cyclic fold . Further bifurcations of 4T lead to cross-well chaos (point 4, Fig 13.e), coexisting with 3T LO attractor. The symmetry of the 3T LO attractor, corresponding to point 5 can be observed in Fig 13.f. This attractor coexists with 1T SO attractor, which has regained stability in the (inverse) subcritical period doubling. The unsymmetric LO 3T, born in SB bifurcation from the symmetric orbit, (point 6) is displayed in Fig 13.g. It coexists with the still present 1T SO attractor. The unsymmetric LO undergoes period doubling - the corresponding 6T LO attractor (Point 7) also coexists with 1T SO and is shown in Fig 13.h. For lower frequencies another chaotic attractor is born in the period doubling cascade of 1T SO (Point 8,Fig 13.i). The scenario of creation of the latter attractor corresponds to

principal resonance region phenomena.

4.1.3 Remarks

1.) The Melnikov homoclinic function (81), marked in Fig 7. corresponds to the tangle of saddle 1T stable and unstable manifolds. The phenomena were studied experimentally in [1] (direct observation of the manifolds) and in [15] (smooth-fractal basin bifurcations), where satisfactory agreement with Melnikov theory predictions were found. In this paper we show the agreement in the context of the accumulation of folds.

Many phenomena take place in the parameters region close to the curve (81), including the creation and further bifurcations of high period and nonperiodic (chaotic) trajectories. The latter are not attracting yet and can not be observed in simulations. As we see in Fig 7 higher excitations then these given by (81) are required to obtain attracting chaotic orbits.

We do not concentrate on the phenomena close to (81) - they appear in very narrow parameter regions.

2.) We consider now the points in (ν,F) parameter space (Figs 7, also 8-11), where

a.) fold and symmetry breaking

b.) fold and period doubling

of the same orbit seem to coincide.

From the properties of Poincare maps we know that neither the pair a. nor b. can occur in the same point in parameter space (Swift, Wiesenfeld [32]). If it happens in our computations, it is due to the errors of experiment (Fig 7) or approximation (Figs 9-12). The approximation errors are two-fold: firstly, we use different approximate techniques to obtain fold and period doubling (symmetry breaking) instability, secondly, even using consistent, based on Hill's equation, approach we would make errors due to finite representation of solution of (59).

3). The question of one-well chaos ,resulting from period doubling cascade of SO motion, is not discussed here. The phenomenon is observed in very narrow parameter regions (cf Thompson,Bishop and Leung [33]).

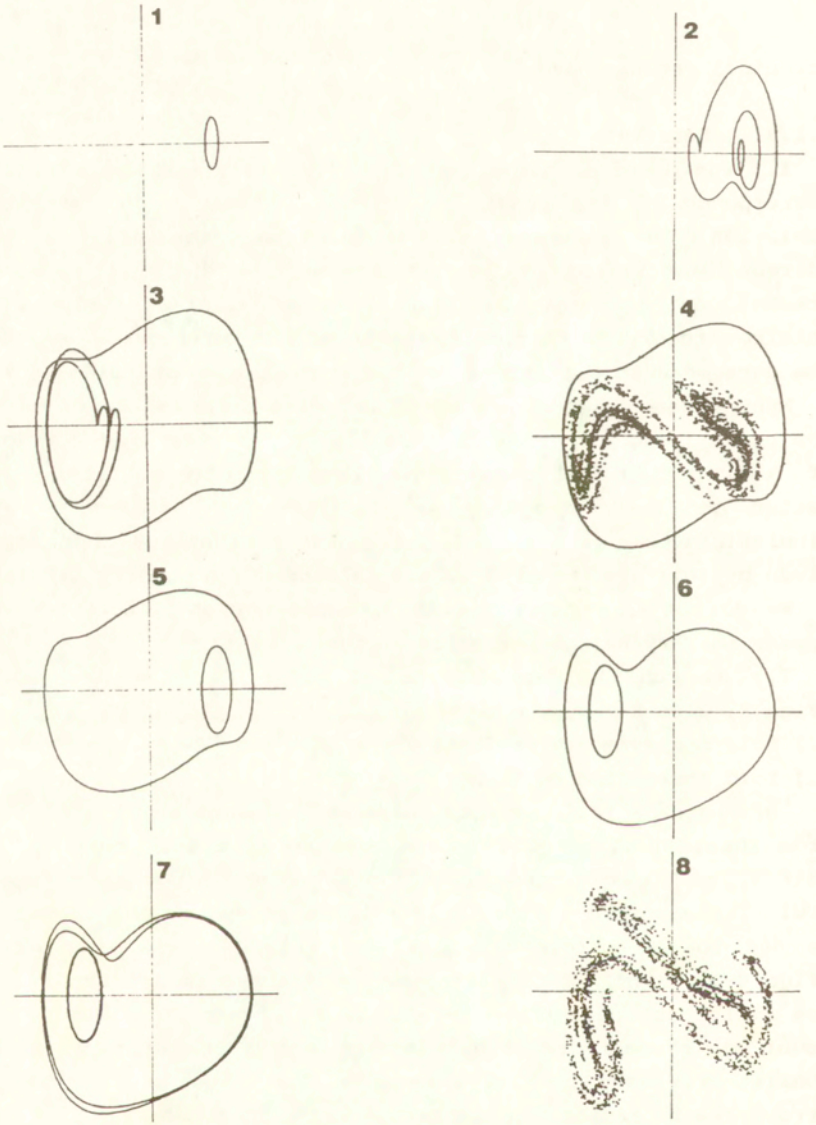

Fig. 12. Various attractors corresponding to the points 1-8

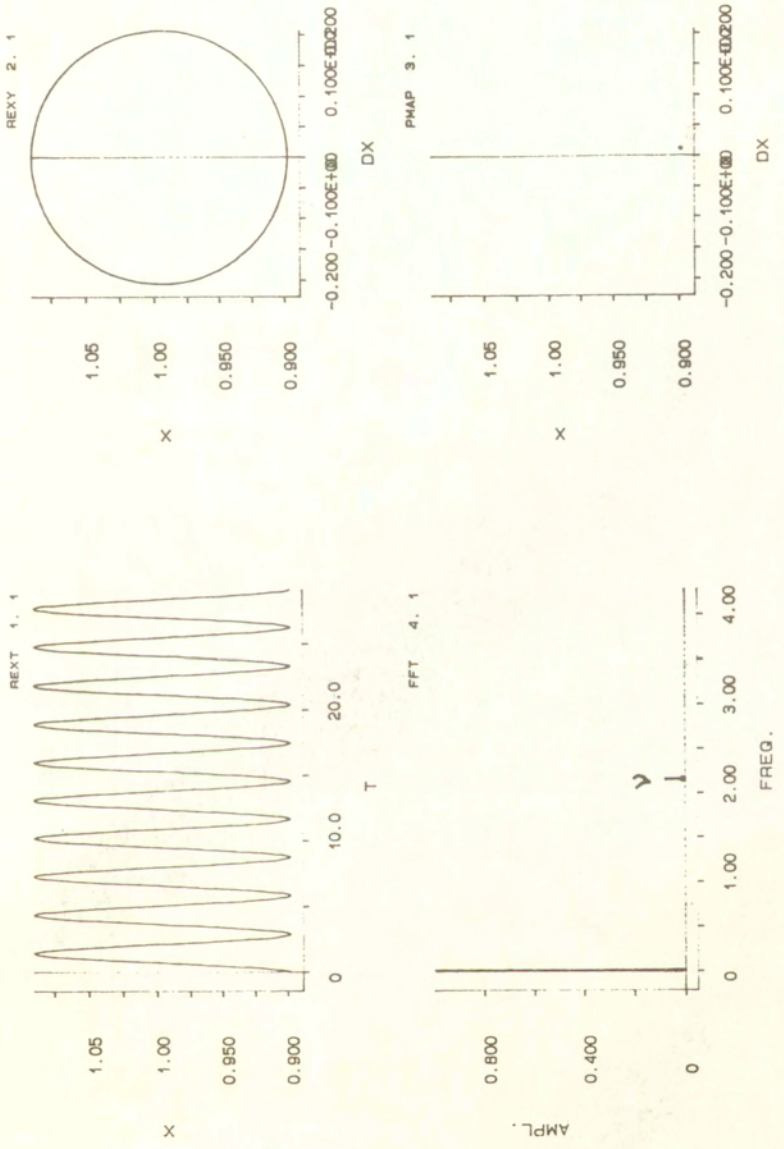

Fig 13. Characteristics of various attractors
Fig. 13.a. Point 1, 1T SO, F=0.35, h=0.1, ν=2.15

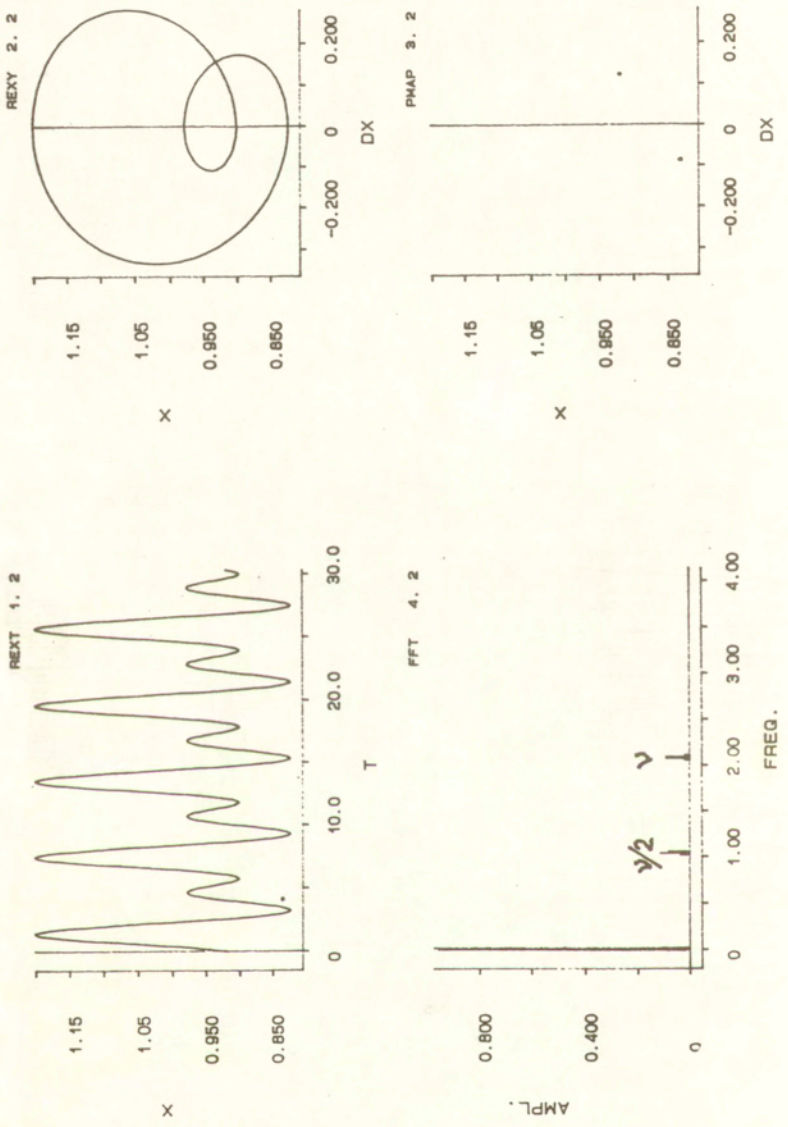

Fig. 13.b. Point 2, 2T SO, F=0.35, h=0.1, ν=2.075

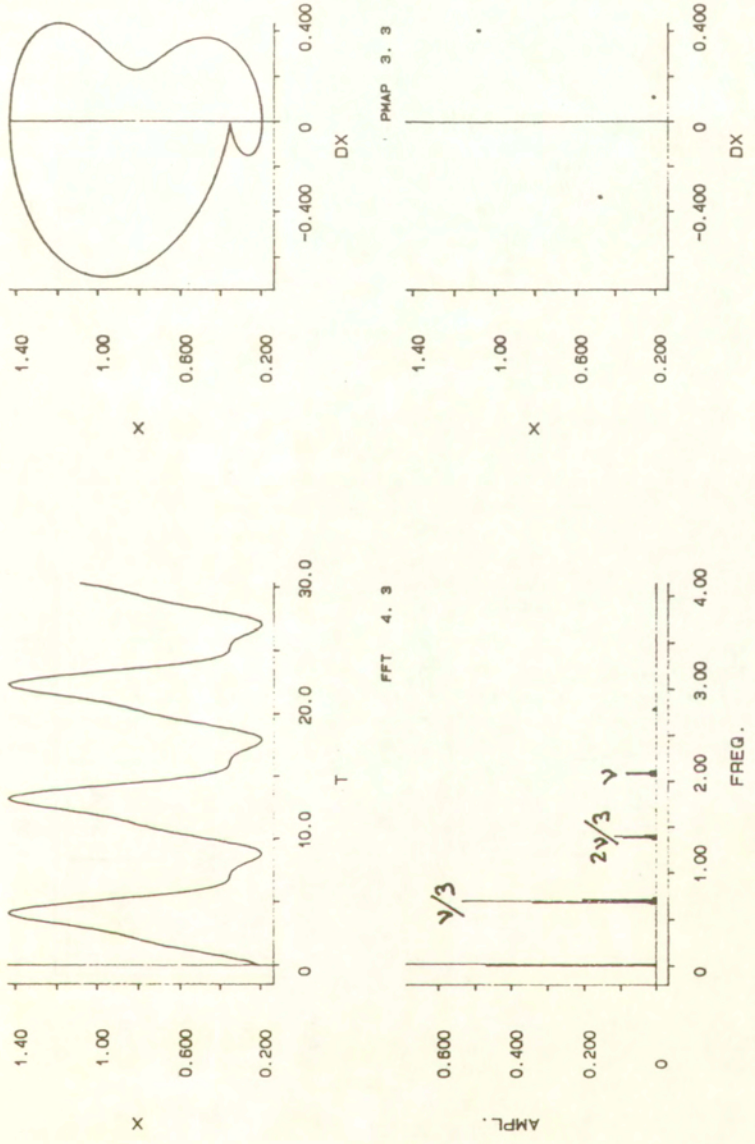

Fig. 13.c. Point 2, 3T SO, F=0.35, h=0.1, ν=2.075

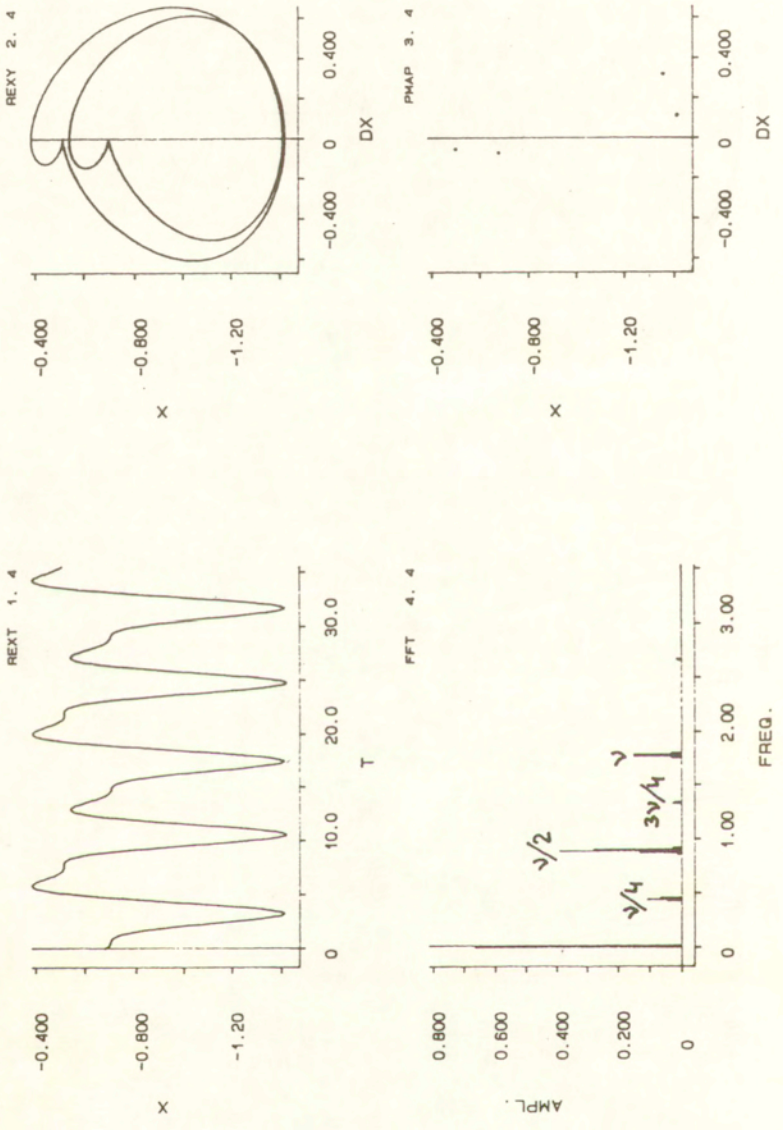

Fig. 13. d. Point 3, 4T SO, F=0.35, h=0.1, ν=1.775

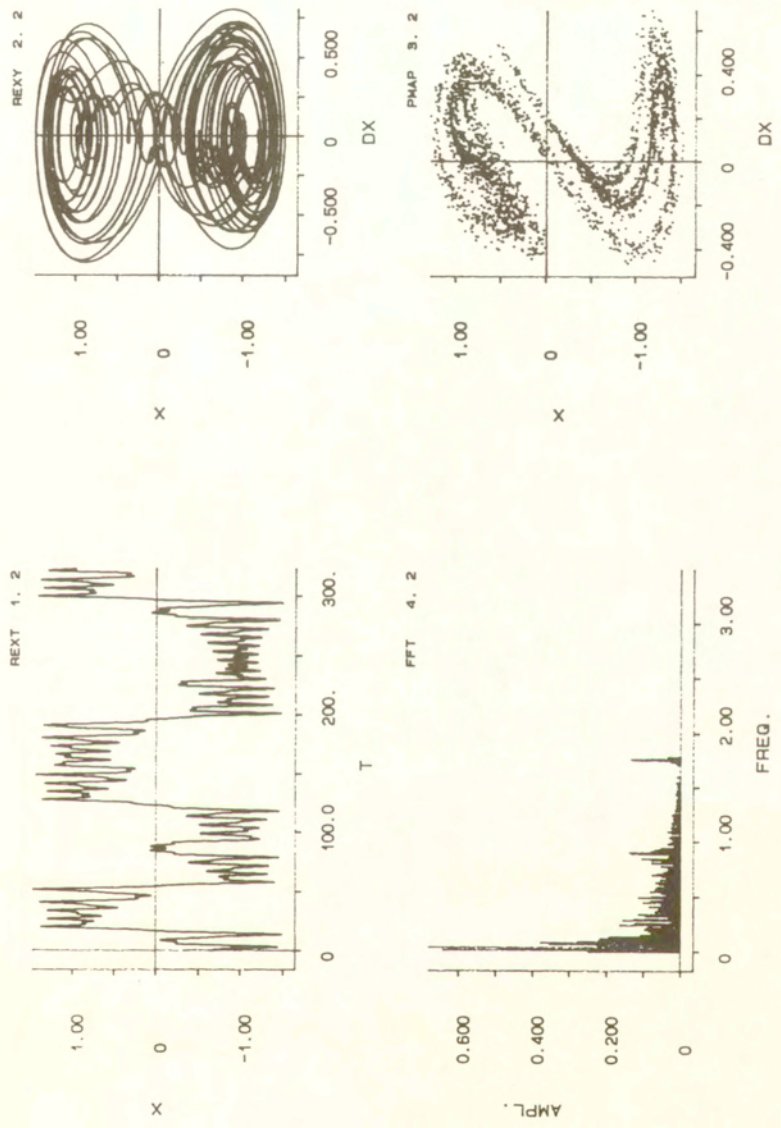

Fig. 13.e. Point 4, Cross-well chaos, F=0.35, h=0.1, ν=1.75

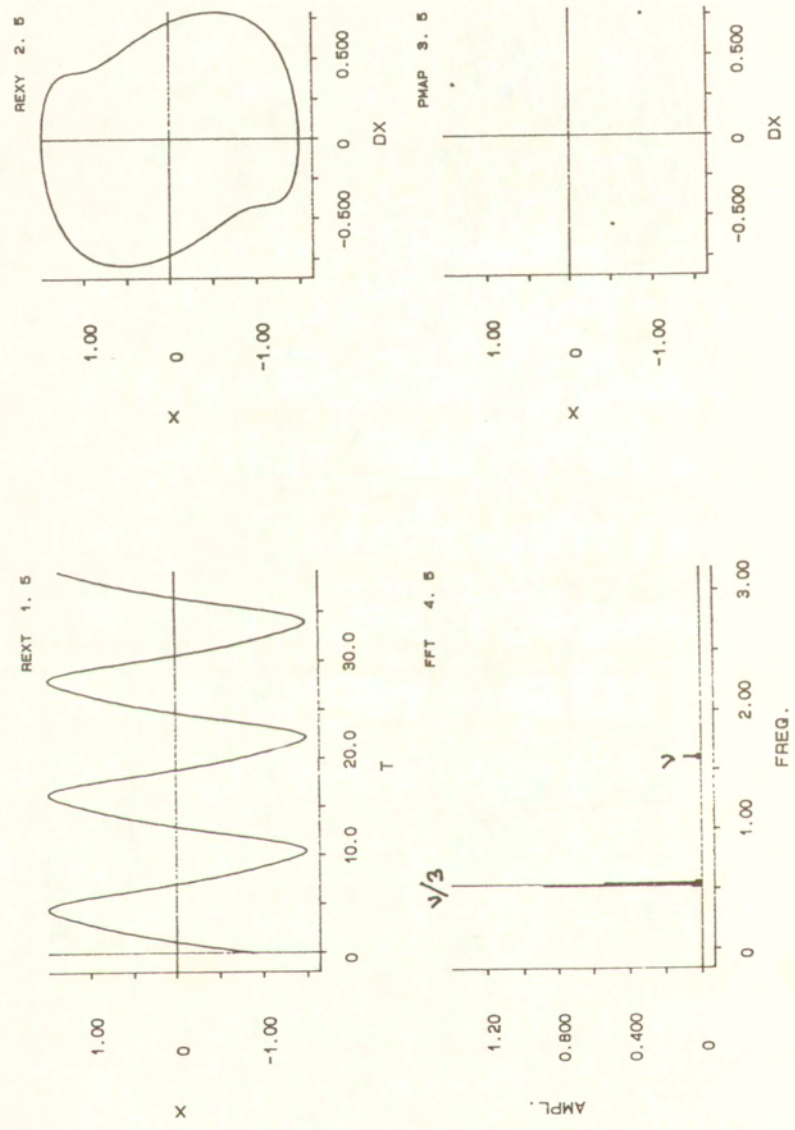

Fig. 13.f. Point 5, Symmetric 3T LO, P=0.35, h=0.1, ν=1.6

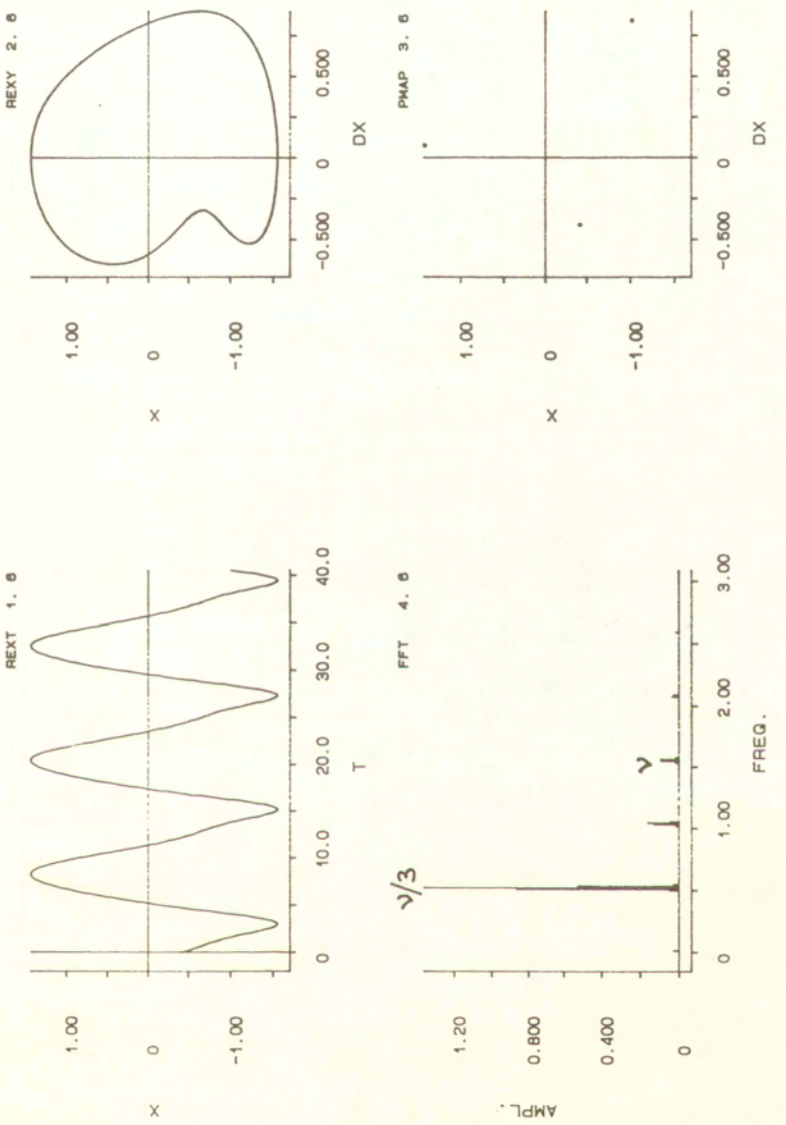

Fig. 13.g. Point 6, Unsymmetric 3T LO, P=0.35, h=0.1, ν=1.55

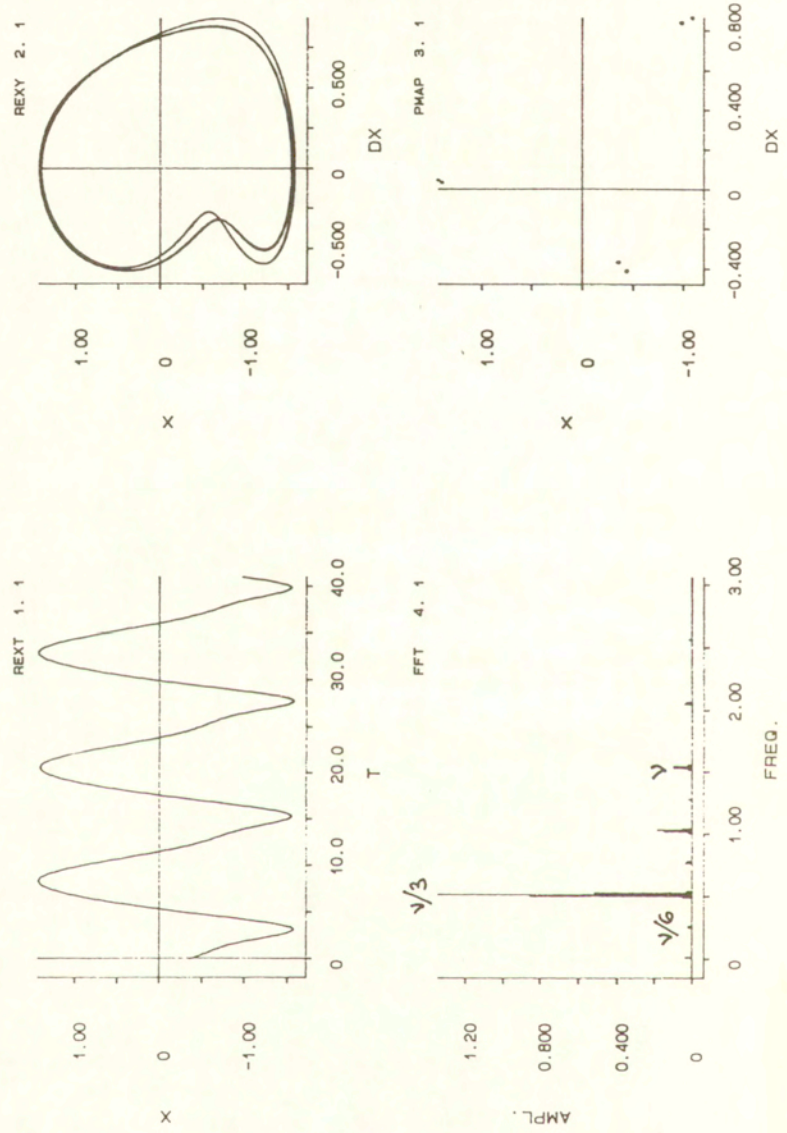

Fig. 13.h. Point 7, 6T LO, P=0.35, h=0.1, ν=1.533

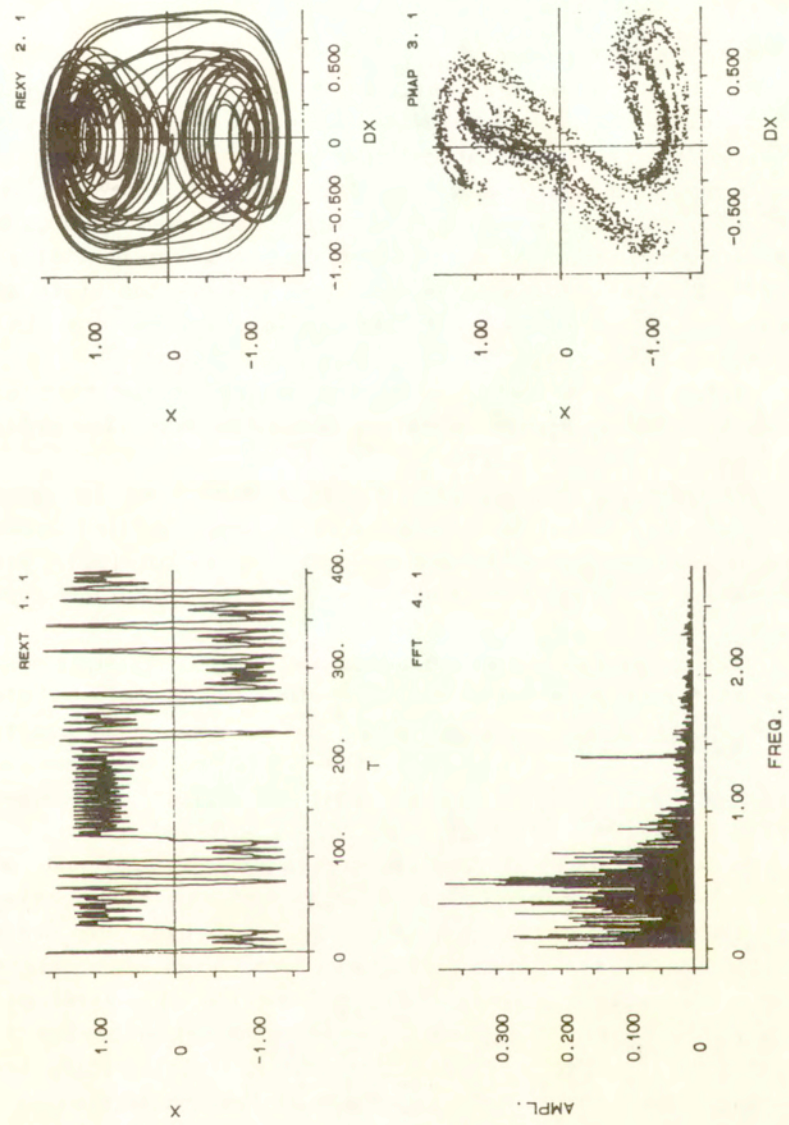

Fig. 13.g. Point 8, Cross-well chaos, P=0.35, h=0.1, ν=1.4

4.2. Escape phenomena

Having described bifurcations of low-order subharmonics we can, basing on numerical evidence, consider other SO motions negligible. Some theoretical results concerning high order subharmonics support this conjecture. Roughly speaking, it can be shown that the width of the regions occupied by high order subharmonics mT in the phase space decreases exponentially with m [7]. Similar exponential estimations concern the width of the regions of existence of high-periodic attractors in the parameter space [24].

Basing on the above assumption we can state that escape points in the parameter space are where the last (low order) SO subharmonic loses stability.

In [20] the bifurcations analysis were used in order to estimate escape and chaos phenomena in the principal resonance region of the parameter space - cf Fig 12 in [20]. Similar phenomena have been found in the subharmonic region and depicted in Fig 14.

We can escape from potential well in two ways: through period-doubling cascade, which results in chaos, or through subcritical period doubling, which causes jump to the chaotic or 3T LO attractor. The analogy with the principal resonance is apparent, with the difference, that there fold of nonresonant orbit is involved in escape, not period doubling.

We illustrate now new scenarios of escape and other discontinuous bifurcations of attractors using experimental amplitude characteristics (Fig 15). The axes of ordinates correspond to the driving frequency, the axes of abscissae to the generalized amplitude of motion, understood as $\bar{a} = (x_{max} - x_{min})/2$. The figure can be compared with Figs 3 and 4 of [20] in order to find differences and similarities between subharmonic, principal and superharmonic resonance regions.

Fig 15.a illustrates the hysteresis between 1T SO attractor and 2T SO orbit, or other orbits bifurcating from 2T in period

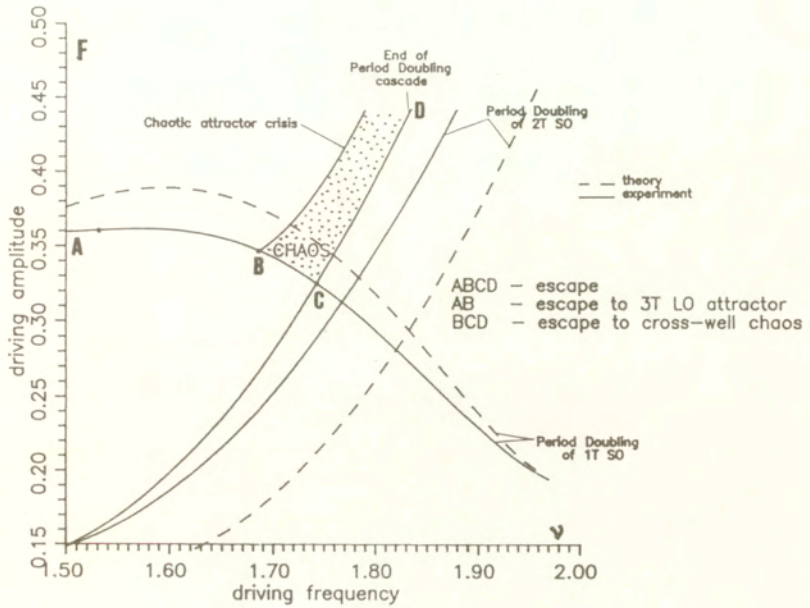

Fig. 14. Escape phenomena in the subharmonic parameters region

doublings. The hysteresis involves two jumps: up (subcritical period doubling of 1T SO) and down (end of period doubling cascade of 2T SO). We emphasize the similarity to Fig 3.b in [20].

In 15.b period doubling cascade of 2T SO results at decreasing ν in a jump up and cross-well chaos that persists in a short range of frequencies. The chaotic attractor disappears further for the frequency corresponding to subcritical PD of 1T and is replaced by 1T attractor. This process is invertible ie increasing frequency we jump back to chaos without a hysteresis. The scenario resembles the situation in the p rincipal resonance region, where the chaotic attractor disappears (or occurs) for the frequency corresponding to the fold of nonresonant orbit

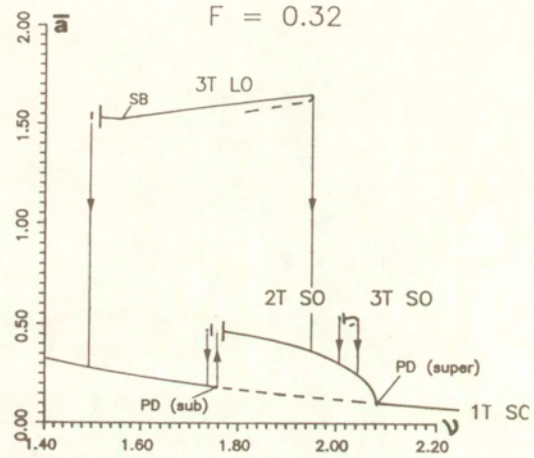

Fig 15.a

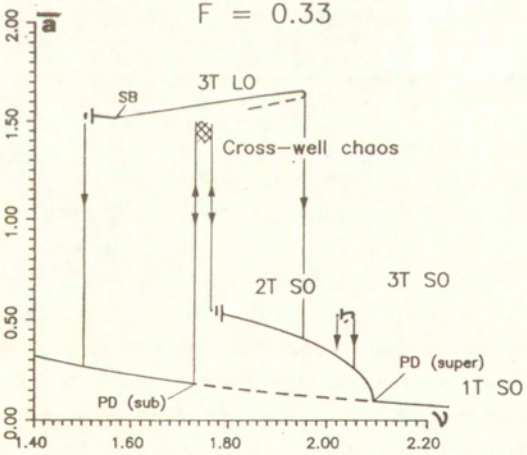

Fig. 15.b

Fig. 15. Experimental resonance curves

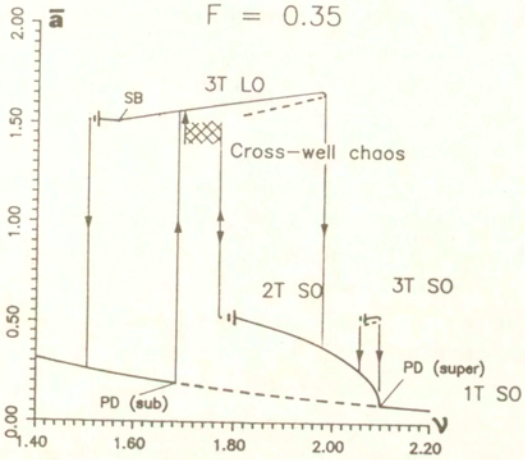

Fig. 15.c

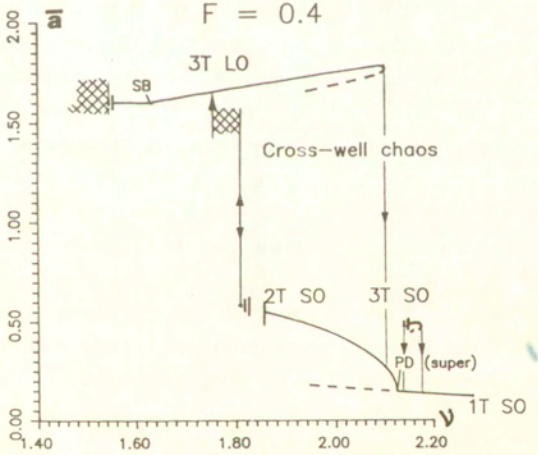

Fig. 15.d

(Fig 3.c in [20]). The common factor in these two situations is that a stable regular solution appears and destroys the chaotic attractor. The scenario seems to be of subduction type [23]. The LO attractor does not take part in the bifurcations, which involve the chaotic orbit.

If we increase ν in Fig 15.c the subcritical period doubling of 1T SO causes a jump to 3T LO. Further increasing ν results in the motion along LO resonance curve, terminating in the jump down to 2T SO. Now decreasing frequency we can go through period doubling cascade resulting in chaotic motion and find ourselves again on the LO branch due to the chaotic attractor destruction. This destruction differs from Fig 15.b case. We do not associate it with instability of any low-periodic solution. It is also not invertible (we can pass back from 1T LO to chaos, but we must move on hysteresis loop). Similar behavior can be observed in the principal resonance region (Figs 3.d,e in [20]). This chaotic attractor catastrophe seems to be of crisis type, involving the collision between the chaotic attractor and an unstable orbit on the basin boundary of this attractor.

The Fig 15.d is similar to 15.c for higher frequencies; for lower ones SO does not exist - only 3T LO passes in period doubling cascade to chaotic cross-well motion, emanating in (ν,F) plane from the region of principal resonance.

In all the Figures 15.a-d the 3T SO attractor is present in a short range of frequencies. We can not jump to this resonance curve from other orbits, but we can fall down from 3T SO to 2T or 1T motion.

We note that in some regions of (ν,F) plane increasing force at ν=const may result in decreasing amplitude (1T SO resonant → 1T SO nonresonant or 2T SO → 1T SO passages).

5. Concluding remarks

1. As we have seen conventional near-linear perturbation techniques can be modified in order to investigate strongly nonlinear phenomena. In this paper we used the modification in

order to obtain LO resonance solutions, leaving for SO motions more classic approach. We believe that modifying also SO analysis we would improve the agreement with experimental results (especially in 1:3 SO case - here the amplitude of motion is relatively large and the classic approach is less useful than in 1:1, 1:2 cases).

2. The perturbation technique together with stability analysis allows us to predict many bifurcations in the parameter space. Concerning the bifurcations of low order subharmonics we can estimate escape regions in parameter space.

3. Near-linear perturbation methods complement Melnikov theoretical approach. They can yield more details concerning low-order resonances, which are dominant from the physical point of view. The near-Hamiltonian approach is more suitable for the analysis of phenomena neighbouring with the homoclinic bifurcation.

4. We have shown that many important phenomena may be predicted using analytical methods of local nature. In particular, we turn the attention to the type of chaotic attractor catastrophe, which can be investigated in relation to local events. Another form of catastrophe, known as crisis, is also observed.

REFERENCES

1. Holmes,P.J., A Nonlinear Oscillator with a Strange Attractor, Phil. Trans. Roy. Soc. A, 292, 1979, 419-448
2. Holmes,P.J., Moon,F.C., Strange Attractor and Chaos in Nonlinear Mechanics,J. Applied Mechanics, 50, 1983, 1021-1032
3. Tang,D.M., Dowell,E.H.,On the Treshold Force for Chaotic Motions for a Forced Buckled Beam, J. Applied Mechanics, 65, 1979, 190-196

4. Moon,F.C. and Holmes,P.J., A Magnetoelastic Strange Attractor,J. Sound. Vib. 65, 1979, 275-296
5. Mahaffey,R.A., Anharmonic Oscillator Description of Plasma Oscillations, Phys. Fluids 19, 1976, 1387-1391
6. Guckenheimer,J., Holmes,P.J.,Nonlinear Oscillations, Dynamical Systems and Bifurcations of Vector Fields, Springer-Verlag, New York, 1983
7. Wiggins, S., Introduction to Applied Nonlinear Dynamical Systems and Chaos,Springer-Verlag, New York, 1990
8. Greenspan,B.D., Holmes,P.J.,Homoclinic Orbits, Subharmonics and Global Bifurcations in Forced Oscillations, in Nonlinear Dynamics and Turbulence ,Barenblatt,G.I., Ioos,G., Joseph,D.D. (eds) Pitman, Boston, 1983
9. Wiggins, S., Chaotic Transport in Dynamical Systems, Springer-Verlag, New York, 1992
10. Neihstadt,A., Probability Phenomena Due to Separatrix Crossing, Chaos 1, 1991, 42-48
11. Ueda, Y.,Steady motions exhibited by Duffing's equation: a picture book of regular and chaotic motions, New Approaches to Non-Linear Problems in Dynamics, SIAM, Philadelphia, 1990, 311-322
12. Moon,F.C., Li,G.-X., The Fractal Dimension of the Twin-Well Potential Strange Attractor, Physica D, 17, 1985, 99-108
13. Arecchi,F.T., Lisi,F., Hopping Mechanism Generating 1/f Noise in Nonlinear Systems, Phys. Rev. Lett., 49, 1982, 94-98
14. Gafka,D., Tani,J., Chaos in Multi-Well Potential Magnetoelastic Systems, Rep. Inst. Fluid Sci., Tohoku Univ., 1991, 3, 1-17
15. Moon,F.C., Li,G.-X., Fractal Basin Boundaries and Homoclinic Orbits for Periodic Motion in a Two-Well Potential, Phys. Rev. Lett., 55, 1985, 1439-1444
16. Ueda,Y., Yoshida,S., Stewart,H.B. and Thompson, J.M.T., Basin Explosions and Escape Phenomena in the Twin-Well Duffing Oscillator: Compound Global Bifurcations Organizing Behavior, Phil. Trans. R. Soc. A, 332, 1990, 169-186

17. Pezeshki,Ch., Dowell,E.H., On Chaos and Fractal Behavior in a Generalized Duffing's System, Physica D, 32, 1988, 194-204
18. Szemplińska-Stupnicka,W., Cross-Well Chaos and Escape Phenomena in Driven Oscillators, Nonlinear Dynamics 3, 1992, 225-243
19. Szemplińska-Stupnicka,W. and Rudowski,J., Local Methods in Predicting an Occurence of Chaos in the Two-Well Potential System: Superharmonic Frequency Region, J. Sound Vib., 152, 1992, 57-72
20. Szemplińska-Stupnicka,W. and Rudowski,J., Steady States in the Twin-Well Potential Oscillator: Computer Simulations and Approximate Analytical Studies, in print
21. Mc Robie,F.A. and Thompson J.M.T., Criteria for Escape Phenomena in Driven Oscillators Using Melnikov-Like Energy Estimates, in print
22. Abraham,R.H., Stewart,H.B, A Chaotic Blue-Sky Catastrophe in Forced Relaxation Oscillations, Physica D, 21, 1986, 394-400
23. Grebogi,C. and Ott,E. and Yorke,J.A, Crises, Sudden Changes in Chaotic Attractors and Transient Chaos, Physica D, 7, 1983, 181-200
24. Grebogi,C., Ott,E. and Yorke,J.A., Basin Boundary Metamorphoses: Changes in Accessible Boundary Orbits, Physica D, 27, 1987, 243-262
25. Szemplińska-Stupnicka,W., The Behavior of Nonlinear Vibrating Systems, vol.I, Kluwer Academic Publishers, Dordrecht, 1990
26. Bogolyubov,N., Mitropolsky,Y., Asymptotic Methods in the Theory of Nonlinear Oscillators, Gordon and Breach Science Publication, New York, 1961
27. Nayfeh,A.H., Introduction to Perturbation Techniques, Wiley, New York, 1981
28. Bolotin,V.V, Dynamic Stability of Elastic Systems, Holden-Day, San Francisco, 1964
29. Meirovitch, L., Methods of Analytical Dynamics, McGraw-Hill, New York, 1970

30.Hayashi, Ch., Nonlinear Oscillations in Physical Systems, Princeton University Press, Princeton,N.Y., 1985

31.Räty,R., von Boehm,J., Isomäki,H.M., Absence of Inversion-Symmetric Limit Cycles of Even Periods and the Chaotic Motion of Duffing's Oscillator, Phys. Letters, 1984, 103A, 289-292

32.Swift,J., Wiesenfeld,K., Suppression of Period Doubling in Symmetric Systems, Phys. Rev. Lett., 52, 1984, 705-712

33.Thompson, J.M.T., Bishop, S.R., Leung,L.,M., Fractal Basins and Chaotic Bifurcations Prior to Escape from a Potential Well, Phys. Letters, 121A, 1987, 116-120

ACKNOWLEDGMENT

This work was supported by Grant No. 3 3303 92 03 with funds provided by Komitet Badań Naukowych in the years 1992-1994.